



ELECTROENCEPHALOGRAM DATA PLATFORM FOR APPLICATION OF REDUCTION METHODS

Ana Carolina Gomes de Almeida Albuquerque

Dissertação de Mestrado apresentada ao Programa de Pós-graduação em Engenharia Biomédica, COPPE, Universidade Federal do Rio de Janeiro, como parte dos requisitos necessários à obtenção do título de Mestre em Engenharia Biomédica.

Orientadores: Maurício Cagy

Carlos Julio Tierra Criollo

Rio de Janeiro

Junho de 2019

ELECTROENCEPHALOGRAM DATA PLATFORM FOR APPLICATION OF
REDUCTION METHODS

Ana Carolina Gomes de Almeida Albuquerque

DISSERTAÇÃO SUBMETIDA AO CORPO DOCENTE DO INSTITUTO ALBERTO
LUIZ COIMBRA DE PÓS-GRADUAÇÃO E PESQUISA DE ENGENHARIA
(COPPE) DA UNIVERSIDADE FEDERAL DO RIO DE JANEIRO COMO PARTE
DOS REQUISITOS NECESSÁRIOS PARA A OBTENÇÃO DO GRAU DE MESTRE
EM CIÊNCIAS EM ENGENHARIA BIOMÉDICA.

Examinada por:

Prof. Maurício Cagy, D.Sc.

Prof. Roberto Macoto Ichinose, D.Sc.

Prof. Eduardo Jorge Custódio da Silva, PhD.

Prof. Mario Junior Fiorani, PhD.

RIO DE JANEIRO, RJ - BRASIL

JUNHO DE 2019

Albuquerque, Ana Carolina Gomes de Almeida

Electroencephalogram Data Platform for Application of
Reduction Methods / Ana Carolina Gomes de Almeida
Albuquerque. – Rio de Janeiro: UFRJ/COPPE, 2019.

XVI, 87 p.: il.; 29,7 cm.

Orientadores: Maurício Cagy

Carlos Julio Tierra Criollo

Dissertação (mestrado) – UFRJ/ COPPE/ Programa de
Engenharia Biomédica, 2019.

Referências Bibliográficas: p. 68-81.

1. Hilbert Amplitude-integrated Electroencephalography. 2.
Amplitude-integrated Electroencephalography. 3. EEG
Database for Epileptic Seizure Detection. I. Cagy, Maurício
et al. II. Universidade Federal do Rio de Janeiro, COPPE,
Programa de Engenharia Biomédica. III. Título.

Dedicatória

Este trabalho é dedicado a todos aqueles com epilepsia, seus cuidadores, familiares e aqueles que se dedicam na busca de tratamentos e técnicas que possam melhorar a qualidade de vida destas pessoas.

Agradecimentos

À minha família, pelo suporte e compressão. Em especial, a meus avós, pelo incansável incentivo e exemplo.

Aos orientadores, Maurício Cagy e Carlos Julio Tierra-Criollo pela paciência, sabedoria e atenção que dividiram neste trabalho.

A todo corpo docente e discente do Programa de Engenharia Biomédica da Universidade Federal do Rio de Janeiro.

Agradeço a FAPERJ, CAPES, CNPq e FINEP pelo apoio financeiro a mim e ao meu programa, sem o qual este trabalho não poderia ter sido realizado.

Resumo da Dissertação apresentada à COPPE/UFRJ como parte dos requisitos necessários para a obtenção do grau de Mestre em Ciências (M.Sc.)

PLATAFORMA DE DADOS DE ELETROENCEFALOGRAMA PARA
APLICAÇÃO DE MÉTODOS DE REDUÇÃO DE DADOS

Ana Carolina Gomes de Almeida Albuquerque

Junho/2019

Orientadores: Maurício Cagy

Carlos Julio Tierra Criollo

Programa: Engenharia Biomédica

O eletroencefalograma (EEG) de longa duração (≥ 24 -h) em monitoramento contínuo é diferencial no diagnóstico e classificação de eventos epileptiformes, como crises não convulsivas e *status epilepticus*, em pacientes de Unidades de Tratamento Intensivo (UTI). Este exame requer métodos objetivos de análise, redução e transmissão de dados. O objetivo desse trabalho é avaliar a especificidade e a sensibilidade dos métodos HaEEG e aEEG em combinação com EEG multicanal convencional na detecção de eventos epileptiformes. Uma arquitetura de integração de dados foi projetada para gerir o armazenamento, processamento e análise de dados de EEG. Foram utilizados dados do banco de dados de EEG público do CHB-MIT. O sinal reduzido foi obtido pela segmentação do envelope do EEG, com percentis 10 e 90 obtidos para cada segmento. A aplicação do filtro assimétrico (2-15 Hz) e em bandas clínicas (1-70 Hz) foi comparada. Os limiares superiores e inferiores dos segmentos do aEEG e HaEEG foram usados para classificar épocas ictais e não ictais. A classificação foi comparada com as anotações feitas por um especialista para cada paciente. As medianas das frequências instantâneas para períodos ictais e não ictais foram analisadas com *Wilcoxon Rank Sum Test* com significância para filtragem assimétrica ($p = 0,0055$), mas não nas bandas clínicas ($p = 0,1816$).

Abstract of Dissertation presented to COPPE/UFRJ as a partial fulfillment of the requirements for the degree of Master of Science (M.Sc.)

ELECTROENCEPHALOGRAM DATA PLATFORM FOR APPLICATION OF REDUCTION METHODS

Ana Carolina Gomes de Almeida Albuquerque

June/2019

Advisors: Maurício Cagy

Carlos Julio Tierra Criollo

Department: Biomedical Engineering

Long-term electroencephalogram (EEG) monitoring (≥ 24 -h) is a resourceful tool for properly diagnosis sparse life-threatening events like non-convulsive seizures and status epilepticus in Intensive Care Unit (ICU) inpatients. Such EEG data requires objective methods for data reduction, transmission and analysis. This work aims to assess specificity and sensibility of HaEEG and aEEG methods in combination with conventional multichannel EEG when achieving seizure detection. A database architecture was designed to handle the interoperability, processing, and analysis of EEG data. Using data from CHB-MIT public EEG database, the reduced signal was obtained by EEG envelope segmentation, with 10 and 90 percentiles obtained for each segment. The use of asymmetrical filtering (2-15 Hz) and overall clinical band (1-70 Hz) was compared. The upper and lower margins of compressed segments were used to classify ictal and non-ictal epochs. Such classification was compared with the corresponding specialist seizure annotation for each patient. The difference between medians of instantaneous frequencies of ictal and non-ictal periods were assessed using Wilcoxon Rank Sum Test, which was significant for signals filtered from 2 to 15 Hz ($p = 0.0055$) but not for signals filtered from 1 to 70 Hz ($p = 0.1816$).

TABLE OF CONTENTS

LIST OF FIGURES	xi
LIST OF TABLES	xiv
LIST OF ABBREVIATIONS AND ACRONYMS	xv
1 INTRODUCTION	1
1.1 PURPOSE OF THE STUDY	4
1.1.1 General goal.....	4
1.1.2 Specific goals.....	4
1.2 SIGNIFICANCE OF THE STUDY	4
1.3 ORGANIZATION OF THE STUDY.....	5
2 BACKGROUND	7
2.1 EPILEPSIES	7
2.1.1 Definition.....	7
2.1.2 Epidemiology of Epilepsy	9
2.1.3 Diagnostic Axes.....	10
2.2 EEG	11
2.2.1 Epileptic Activity in Electroencephalography.....	12
2.3 DATA REDUCTION TECNHIQUES	14
2.3.1 Amplitude-integrated Electroencephalography (aEEG).....	14
2.3.1.1 Classification and Interpretation of aEEG.....	15
2.3.1.2 Data acquisition	19
2.3.1.3 Signal Filtering	20
2.3.1.4 Signal Envelope.....	21
2.3.1.5 Signal Reduction	22
2.3.2 Hilbert Amplitude-integrated Electroencephalography (HaEEG)	23

2.3.2.1 Hilbert Transform and analytic signal	23
2.3.2.2 Computation of Hilbert aEEG	24
2.3.2.2.1 Signal Filtering	25
2.3.2.2.2 Signal Envelope	26
2.3.2.2.3 Signal Reduction.....	26
2.3.2.3 Instantaneous Frequency Estimation	27
2.4 PERFORMANCE METRICS	29
2.4.1 Accuracy, Sensibility and Specificity.....	29
2.4.2 ROC Curve	30
2.5 EEG DATA INTEGRATION PLATFORM.....	31
2.5.1.1 Platform Design.....	31
2.5.1.2 EEG Recordings Metadata	32
3 LITERATURE REVIEW	34
3.1 DATA ANALYSIS AND SEIZURE DETECTION.....	34
3.2 EEG DATA INTEGRATION PLATFORM.....	37
3.2.1 Electroencephalogram Database	38
4 MATERIALS AND METHODS	41
4.1 CASUISTRY	41
4.1.1 EEG Data.....	41
4.2 INTEGRATION AND PRE-PROCESSING DATA	43
4.2.1 Data Processing and Orchestration.....	43
4.2.2 Electroencephalogram database	44
4.2.3 Client application.....	44
4.3 EEG SIGNAL PROCESSING	44
4.3.1 Filtering Data.....	44

4.3.2 Envelope Extraction	46
4.3.3 Envelope Compression	48
4.3.4 Selection of ictal segments	49
4.3.5 Analysis of Instantaneous Frequency	53
5 RESULTS	54
5.1.1 Selection of ictal segments	54
5.1.2 Analysis of Instantaneous Frequency	61
5.1.3 Electroencephalogram Data Platform.....	63
6 DISCUSSION.....	65
7 CONCLUSION	67
7.1 PURPOSE AND CONTRIBUTION	67
7.2 FUTURE WORK	67
8 BIBLIOGRAPHY	68
APPENDIX A - Hilbert Transform and Analytic Signal	82
APPENDIX B - CHB-MIT EEG Recordings Montage	84
APPENDIX C - CHB-MIT EEG patients summarized information.....	87

LIST OF FIGURES

Figure 2.1 – The standard 10-20 system of electrode placement at right. At left, modified for neonates nine scalp positions typically used for neonates were highlighted. Public domain modified.

Figure 2.2 – Schematic diagram of aEEG signal processing algorithm. A. Filtered EEG asymmetrically from 2 to 15 Hz; B. rectified EEG signal; C. Rectified signal envelope, with maximum (red) and minimum (green) in each 15-s epoch. D. Time, compressed envelope. E. Amplitude-time compressed envelope F. Compact aEEG tracing. (Adapted from (ZHANG and DING, 2013), under a Creative Commons Attribution license.)

Figure 2.3 – Abnormal aEEG tracings for seizures caused by primary carnitine deficiency in neonate infant (Adapted from (ZHANG and DING, 2013), under a Creative Commons Attribution license).

Figure 2.4 – aEEG commonly used electrode placements. A. Parietal electrodes (P3-P4); B. C3-P3 and C4-P4 electrodes. C. Recommended positions for two-channel bilateral recording on neonates (F3-P3/F4-P4).

Figure 2.5 – Schematic diagram of the frequency response of the asymmetric filter used in analog CFM (Adapted from (ZHANG and DING, 2013), under a Creative Commons Attribution license).

Figure 2.6 – HaEEG for parietal electrodes (P3-P4).for signal filtered at asymmetrical band (2-15 Hz). Adapted from (DE MELO et al., 2014).

Figure 2.7 – HaEEG for parietal electrodes (P3-P4).for signal filtered at overall clinical band (1-70 Hz). Adapted from (DE MELO et al., 2014).

Figure 2.8 – HaEEG envelope acquisition for 15-s ictal segment. A. rectified signal B. envelope acquired from analytic signal using HT (Adapted from de Melo (2015)).

Figure 4.1 – Power Spectral Density of 1 hour of a non-seizure record for subject chb01 A. EEG raw data B. signal filtered at multiples of 16 Hz and 60 Hz.

Figure 4.2 – Data integration architecture.

Figure 4.3 – Frequency response for aEEG asymmetric filter

Figure 4.4 – Example of 30s seizure epoch for chb03 subject filtered from 2 to 15 Hz.

Figure 4.5 – Example of 30s seizure epoch for chb03 subject filtered from 1 to 70 Hz.

Figure 4.6 – Envelope detection for 15-s seizure epoch of chb03 subject for C3-P3 derivation: (a) signal filtered from 2 to 15 Hz (b) envelope acquisition through low-pass filtering (c) envelope detection acquired from Hilbert Transform and analytic signal.

Figure 4.7 – Frequency response for Low Pass Filter used for envelope extraction in aEEG algorithm.

Figure 4.8 – HaEEG (red) and aEEG (yellow) signal processing workflow and calculation parameters of algorithms for analysis within the asymmetrical band filtering (2-15 Hz) and the overall clinical band (1-70 Hz).

Figure 4.9 – Distribution of maximum (bellow) and minimum (above) margin values of HaEEG and aEEG tracing acquired from for seizure segments filtered from 2 to 15 Hz. Figures at right side are zoomed versions of those at the left side. Figure 5.1 – ROC Classification of Ictal HaEEG segments of all subjects for signals filtered within 1-70 Hz (left) and 2-15 Hz (right).

Figure 4.10 – Distribution of maximum (bellow) and minimum (above) margin values of HaEEG and aEEG tracing acquired from for non-seizure segments filtered from 2 to 15 Hz. Figures at right side are zoomed versions of those at the left side.

Figure 4.11 – Distribution of maximum (bellow) and minimum (above) margin values of HaEEG and aEEG tracing acquired from for seizure segments filtered from 1 to 70 Hz. Figures at right side are zoomed versions of those at the left side.

Figure 4.12 – Distribution of maximum (bellow) and minimum (above) margin values of HaEEG and aEEG tracing acquired from for non-seizure recordings filtered from 1 to 70 Hz. Figures at right side are zoomed versions of those at the left side.

Figure 4.13 – Schematic representation of segment classification according to threshold pair values. Epochs classified as ictal segments were highlighted (dash lines).

Figure 5.2 – ROC Classification of Ictal aEEG segments for all subjects for signals with asymmetrical filtering.

Figure 5.3 – ROC Classification of Ictal segments according to age group for HaEEG for signals filtered within 1-70 Hz (left) and 2-15 Hz (right). A. subjects of 1.5-3.5 years age group. B. subjects of 6-9 years age group; C. subjects of 10-13 years age group; D subjects of 14-16 years age group; E. subjects of 18-19 years age group.

Figure 5.4 – ROC Classification of Ictal segments according to age group for aEEG with asymmetrical filtering 2-15 Hz. A. subject of 1.5-3.5 years age group. B. subjects of 6-9 years age group; C. subjects of 10-13 years age group; D subjects of 14-16 years age group; E. subjects of 18-19 years age group.

Figure 5.5 – Distribution of median of instantaneous frequencies acquired from for seizure (left) and non-seizure segments (right) recordings filtered from 2 to 15 Hz.

Figure 5.6 – Distribution of median of instantaneous frequencies acquired from for seizure (left) and non-seizure segments (right) recordings filtered from 1 to 70 Hz.

Figure 5.7 – Database design scheme.

Figure 5.8 – Example of register form of Database client application.

LIST OF TABLES

Table 2.1 – aEEG classification according to voltage criterion

Table 2.2 – aEEG background patterns proposed classification for Preterm and Term Infants based on EEG terminology

Table 2.3 – Confusion matrix for a binary classifier

Table 3.1 – EEG data collections for epilepsy available research per region

Table 4.1 – Quartiles for distribution of maximum and minimum margin of seizure and non-seizure segments

Table 5.1 – Summarized performance metrics for aEEG and HaEEG methods.

Table 5.2 – Summarized performance metrics for aEEG and HaEEG methods analyzed with asymmetrical filtering and clinical band filtering for each age group.

LIST OF ABBREVIATIONS AND ACRONYMS

aEEG – Amplitude-integrated Electroencephalography

ACNS – American Clinical Neurophysiology Society

AUC – Area Under the Curve

CAPES – Coordenação de Aperfeiçoamento de Pessoal de Nível Superior

CFM – Cerebral Function Monitor

CNPq – Conselho Nacional de Desenvolvimento Científico e Tecnológico

DHT – Discrete Hilbert Transform

DSA – Density Spectral Array

EDF – European Data Format

EEG – Electroencephalogram

EPILEPSIAE – Evolving Platform for Improving the Living Expectations of Patients Suffering from IctAI Events

FAPERJ – Fundação de Amparo à Pesquisa do Estado do Rio de Janeiro

FINEP – Financiadora de Estudos e Projetos

HaEEG – Hilbert Amplitude-integrated Electroencephalography

HMM– Hidden Markov Model

HT – Hilbert Transform

IBE – International Bureau for Epilepsy

IED – Interictal Epileptic Discharges

iEEG – intracranial Electroencephalogram

ICU – Intensive Care Unit

ILAE – International League Against Epilepsy

LKS – Landau-Kleffner syndrome

NICU – Neonatal Intensive Care Unit

PHI – Protected Health Information

ROC – Receiver Operating Characteristic

SE – Status Epilepticus

SEF – Spectral edge frequency

SUDEP – Sudden Unexpected (or Unexplained) Death in Epilepsy

1 INTRODUCTION

The Electroencephalogram (EEG) reflects cerebral activity and is a fundamental resource in the treatment and diagnosis of convulsive diseases, sleep disorders, comatose state and dementias (NIEDERMEYER and SILVA, 2005). As a valuable diagnostic procedure, EEG features have been evaluated by an increasingly number of studies that aim at enhancing detection capabilities and effectiveness. Such studies are motivated both by improving quality of life in affected patients and by decreasing brain-related illness economic onus, which reached more than \$2T/yr. in 2014 (HARATI *et al.*, 2014).

One of the most widely used EEG applications is the classification of epilepsy and the therapeutic monitoring of epileptic patients. Such disease is characterized by the predisposition to occurrence of recurrent unprovoked epileptic seizures (two or more) (ILIESCU and CRAIU, 2013). Therefore, a consensual definition for epileptic seizure is “a transient occurrence of signs and/or symptoms due to abnormal excessive or synchronous neuronal activity in the brain” (FISHER *et al.*, 2005).

Indeed, this encephalopathy is refereed as the fourth most common one in the United States and one of the ten most common causes of premature death caused by brain disease in Europe (HIRTZ *et al.*, 2007; OLESEN and LEONARDI, 2003). However, the incidence of epilepsy may differ between developing and industrialized countries (BANERJEE and HAUSER, 2008).

Furthermore, the International League Against Epilepsy (ILAE) conceptual definition for epilepsy acknowledges the impact of this condition on patients’ lives as it is characterized both by such predisposition to generate epileptic seizures and by psychosocial, cognitive and neurobiological dimensions of the disease (FISHER *et al.*, 2014). Hence, it is essential to pursue a conclusive investigation, a proper treatment plan and a prognosis assessment for those with suspected diagnosis of epilepsy (AICARDI and TAYLOR, 2008).

Meanwhile, continuous EEG monitoring is frequently necessary in order to achieve proper classification of seizure type (RIZZUTTI, MUSZKAT e CAMPO, 2001). This resource allows detection of subclinical seizures and ischemia, sedation level

monitoring and therefore supports choice for antiepileptic drugs and optimal therapeutic course (AHMED, TAFRESHI and LANGARI, 2008; ILIESCU and CRAIU, 2013; KENNEDY and GERARD, 2012).

Moreover, nearly one third of the patients continue to experiment insufficiently controlled seizures despite of gold standard treatment. Thus, seizure prediction features are highlighted as a promising option to establish new therapeutic strategies (IHLE *et al.*, 2012).

However, the duration of those EEG records may have from 20 minutes to several hours, depending on the indication (BLUM and RUTKOVE, 2007). Besides, the EEG file size depends on sampling rate, recording duration and channel numbers. Thus, one hour of data record can demand about 50 MiB (for 32-channel EEG sampled at 200 Hz) or nearly 1 GiB (for video EEG, according to data resolution and compression). Hence, long duration records (24h of recording with 32 channels), demand about 2 GiB, for data storage. Likewise, long duration video data can demand 8 to 30 GiB, depending on data resolution and compression (SCHOMER and SILVA, 2010).

Nevertheless, bedside long-term EEG monitoring is also a common resourceful diagnostic tool as it remains a gold standard for seizure detection, quantification and classification (HELLSTRÖM-WESTAS *et al.*, 2008). Hence, montage and trending variations, such as amplitude-integrated EEG (aEEG), have been applied to support clinical decisions in Intensive Care Unit (ICU) (HELLSTRÖM-WESTAS *et al.*, 2008). Furthermore, simultaneously application of aEEG and conventional EEG enhance high-frequency, long lasting and central region-generated seizures detection (GLASS *et al.*, 2013; ZHANG e DING, 2013).

Such reduction method assesses brain function by evaluation of amplitude trends of cerebral activity. This technique can provide important information about cerebral function prior to clinical manifestation. Thus, aEEG trend can improve observation and interpretation by non neuro-physiology specialists physicians and nurses (ZHANG and DING, 2013).

With attention to this background, DE MELO *et al.* (2014; 2015) and DOS SANTOS *et. al* (2017) compared EEG data reduction methods' - aEEG and HaEEG (Hilbert aEEG) - performance when achieving epileptic seizures distinction from

background activity. The HaEEG method is also based on filtered and compressed EEG, although, this algorithm uses the Hilbert Transform (HT) for estimating the signal envelope.

Likewise, HaEEG provides a reduced signal that resembles more reliably the original signal and highlights better seizure segments from background activity when compared to aEEG (DE MELO, *et al.*, 2015; DOS SANTOS *et al.*, 2017).

Those findings lead to further investigations of HaEEG application to identify ictal segments in the EEG of hospitalized patients and for remote data transmission. Thus, automatic detection and classification of events of interest and large data reduction are important techniques to allow analysis, processing and transmission of EEG signals (KENNEDY and GERARD, 2012). The usage of data reduction techniques for signal transmission purpose could also contribute to relieve issues concerning to ICUs specialists distribution and availability (DE MELO *et al.*, 2015).

Additionally, differences in variance values of EEG instantaneous frequency, which is a feature that can be obtained from HT, between ictal segments and background activity at reduced signal still require more analysis (DE MELO, *et al.*, 2015). Furthermore, the measure of inter-observer variability of classifications of ictal patterns using HaEEG and aEEG can also provide important information about accuracy and clinical applications of both methods (AL NAQEEB *et al.*, 1999; DOS SANTOS *et al.*, 2017).

However, further studies are necessary to clarify sensitivity and specificity of HaEEG and aEEG for electrographic seizure detection. Thus, this study aims to determine accuracy, sensitivity and specificity of seizure detection in multiple EEG channel (10-20 international system), from which aEEG and HaEEG can be obtained. Also, such performance metrics are also assessed for analysis of a voltage pattern for HaEEG that could help to achieve proper classification of ictal and background activity.

The application of these techniques to the detection and analysis of epileptic activity can potentially allow early diagnosis, alert providers or triggering treatment protocols. Therefore, this study proposes application of data reduction techniques within an EEG data integration platform, in order to apply such processing methods to signals collected as routine procedures in a hospital environment. To this end, this platform must be able

to handle large amounts of data, performing EEG data crunching as much as to provide processed data, signals, metadata and features that could contribute to diagnostic analysis.

1.1 PURPOSE OF THE STUDY

1.1.1 General goal

Determine accuracy, specificity and sensibility of Hilbert amplitude-integrated Electroencephalography (HaEEG) and Amplitude-integrated Electroencephalography (aEEG) methods in combination with conventional multichannel electroencephalogram (EEG) when achieving seizure detection.

1.1.2 Specific goals

- Evaluate the Amplitude-integrated Electroencephalography (aEEG) and the Hilbert aEEG (HaEEG) performance when achieving epileptic seizures detection based on accuracy, specificity and sensibility values.
- Analyze Amplitude-integrated Electroencephalography (aEEG) and the Hilbert aEEG (HaEEG) amplitude ranges as a criterion for selection of ictal segments.
- Evaluate values of instantaneous frequency obtained from Hilbert Transform for ictal and background segments of the reduced signal.
- Design and implement a de-identified EEG database for research purpose.
- Design and implement architecture of an EEG data platform to allow orchestration of integration and analyzes of EEG data.

1.2 SIGNIFICANCE OF THE STUDY

The present study is motivated by aforementioned background and aims to enhance capacity of EEG interpretation in healthcare system, improving process effectiveness and efficiency. Therefore, decreased diagnostic time is an important factor in treatment response, and assessment of risk of permanent neurological sequelae or mortality. This

efficiency can also mean treatment costs reduction, due to agility and effectiveness improvement in diagnosis process.

Furthermore, the early detection of complications in EEG monitoring of ICU inpatients can prevent serious long-term impairments and reduce ICU stay. Such diagnosis capabilities can also contribute to decrease the brain-related illness economic onus.

In order to achieve the intended goals, an acceptable amount of data to support comprehensive experimentation is required. Nonetheless, literature review suggests that populational data such as epilepsy epidemiologic, social and cultural dimensions and treatment access and features could differ between low- and high-income countries, regardless the similarities in biologic and clinical aspects.

Thus, an integrated Brazilian EEG database is presented as an opportunity for collaboration and research in line with other efforts to provide systemized access to aid neuroscience research.

Hence, for integration of referred data, an EEG data integration platform is required. Such platform allows the orchestration of all processes necessary for data integration, processing and analysis. The purpose of this platform is, therefore, to integrate the hospital facilities and research, development and analysis environment. To that end, both, data collection in referred database and the integration platform will remain available for further clinical research and EEG modeling studies.

1.3 ORGANIZATION OF THE STUDY

The present study aims to evaluate the reliability of electrographic seizure detection by HaEEG and aEEG. To this end, it is organized as follows. Chapter 2 introduces basic concepts and definitions such as epilepsies and data reduction techniques. We first describe definitions and classifications adopted in this study, as well as provide a brief overview of electroencephalogram features. Further, the last section of Chapter 2 reviews requirements for an EEG data integration platform. Chapter 3 summarizes EEG integration efforts and EEG database designed to address

common use diagnostic applications along with a computer-based EEG analysis latest endeavors review.

Subsequently, Chapter 4 provides a breakdown view of signal processing approach, as well as casuistry information of the analyzed data. Besides, a description of the database presented in this study along with its integration processes is given in this chapter. Accordingly, Chapter 5 presents the results that are discussed in next Chapter. Furthermore, Chapter 7 gives a summary of this study as well as a review on directions for future work.

2 BACKGROUND

2.1 EPILEPSIES

2.1.1 Definition

A consensus definition provided for the term *epileptic seizure* by International League Against Epilepsy (ILAE) and the International Bureau for Epilepsy (IBE), in 2005, was a “transient occurrence of signs and/or symptoms due to abnormal excessive or synchronous neuronal activity in the brain” (FISHER *et al.*, 2005). At this time, same consensus characterized epilepsy as a predisposition to generate epileptic seizures (FISHER *et al.*, 2005).

At this time, an operational definition of epilepsy was also provided by ILAE as a disorder characterized by occurrence of at least two unprovoked seizures occurring more than 24-h apart (FISHER *et al.*, 2005). Subsequently, epilepsy was defined operationally by ILAE, in 2014, as brain disease when observed any of the following conditions:

- (1) At least two unprovoked (or reflex) seizures occurring > 24 h apart;
- (2) one unprovoked (or reflex) seizure and a probability of further seizures similar to the general recurrence risk (at least 60%) after two unprovoked seizures, occurring over the next 10 years;
- (3) diagnosis of an epilepsy syndrome (FISHER *et al.*, 2014).

Furthermore, ILAE and IBE agreed that epilepsy to be considered a disease rather than a disorder, as this phrase may bring better understanding about severity of epilepsy (FISHER *et al.*, 2014). At the present study, the latest definition is adopted. Besides, ILAE proposed the phrase “resolved” for individuals whose are considered no longer have epilepsy. However, this definition does not guarantee that the disease will not return (FISHER *et al.*, 2014).

However, an epileptic seizure may be the result of a temporary disturbance in the function of an otherwise normal brain (provoked, acute symptomatic or reactive

seizure) (ENGEL *et al.*, 2008). Hence, misdiagnosis rate of refractory epilepsy can be as high as 26.1% (SMITH *et al.*, 1999). Moreover, common imitators of epilepsy can be psychogenic, nonepileptic seizures and syncope (BHARUCHA *et al.*, 2008).

Meanwhile, a widespread classification divides seizures types as partial or generalized onset, simple or complex partial seizures, and within generalized seizure types (ILAE, 1981). Thereafter, ILAE proposed a multilevel classification based on identification of seizure, epilepsy and epilepsy syndrome type. Within this revised operational framework seizures are categorized as those of focal, generalized or unknown onset. Thus, this classification also encloses subcategories of motor, non-motor, with retained or impaired awareness for focal seizures (FISHER *et al.*, 2017; SCHEFFER *et al.*, 2017). Therefore an updated classification may help diagnostic evaluation in clinical routine and research application (FISHER *et al.*, 2017). For detailed information about such classification the reader is referred to ILAE classification documents.

In addition, a revised definition was also proposed for Status Epilepticus (SE) as “a condition resulting either from the failure of the mechanisms responsible for seizure termination or from the initiation of mechanisms, which lead to abnormally, prolonged seizures (after time point t1 [time point beyond which the seizure should be regarded as ‘continuous’ seizure activity])” (TRINKA *et al.*, 2015). Likewise, such definition highlights two operational dimensions: a time point after which seizure is remarked as a continuous activity (t1) and a another time point (t2) upwards which there is risk of long-term impairment (TRINKA *et al.*, 2015).

Previously, such condition was characterized by an epileptic seizure sufficiently prolonged (≥ 5 min) or by two or more seizures without recovery of consciousness between them (LOWENSTEIN, BLECK and MACDONALD, 1999). An also widespread operational definition for SE describes it as a seizure duration of 30 min which is based on concept that irreversible brain damage may occur after such time of continued seizure activity (TRINKA *et al.*, 2015). Furthermore, TOWNE (1994) suggests an earlier start for SE treatment due prognosis worsens of SE with increasing duration.

Nevertheless, a classification of SE was proposed by ILAE Task Force based on four axes: semiology, etiology, EEG correlates and age, in order to reflect differences of symptoms and signs that may occur between fixed stage of SE and short-lasting seizures (TRINKA *et al.*, 2015).

2.1.2 Epidemiology of Epilepsy

Worldwide prevalence of active epilepsy (patients who have had at least one epileptic seizure within the past five years) was reported by BANERJEE and HAUSER (2008) with a range from 3.6 to 41.3 per 1000. This prevalence in Brazil was described as 11.9:1,000 in greater São Paulo area and as 16.5:1,000 in Porto Alegre (FERNANDES *et al.*, 1993; MARINO *et al.*, 1986). Besides, the lifetime risk for developing epilepsy is described as approximately 3% (KWAN and SANDER, 2004).

However, incidence of epilepsy may differ between developing and developed countries. Hence, in high-income countries the incidence of recurrent unprovoked seizures (age-adjusted epilepsy) ranges from 24 to 53 per 100,000 person-years (BANERJEE and HAUSER, 2008). Although, this incidence for developing countries was described as much higher than in industrialized countries. Namely, at Latin America, age-adjusted epilepsy incidence was described as 77.7–190 per 100,000 people per year (BURNEO *et al.*, 2005). Accordingly, an urban-rural difference in incidence is also reported by HAUSER (2008) in developing countries, as well as poor access to antiepileptic drugs treatment in rural areas.

Moreover, the incidence of epilepsy falls notoriously during adolescence and adult life and rises again in elderly (BANERJEE and HAUSER, 2008). Thus, in a British prospective population-based cohort study, 24% of newly diagnosed or suspected epileptic seizures were 60 years or older (SANDER *et al.*, 1990). Meanwhile, nearly 50% of newly developed epilepsy occurs in childhood or adolescence. Also, sex-specific incidence and prevalence is consistently higher in males than in females in majority of studies (BANERJEE and HAUSER, 2008).

Besides, an incidence-prevalence gap is reported in developing countries, where incidence of epilepsy is higher than high income countries, while prevalence values are

similar worldwide (BHARUCHA *et al.*, 2008). Therefore, age-adjusted prevalence ranges from 2.7 to over than 40 per 1,000 population, although a range between four and eight prevails throughout the world. Nevertheless, greater part of epilepsy cases has no identified cause. However, stroke and trauma were the most common following causes (BANERJEE and HAUSER, 2008; BHARUCHA *et al.*, 2008).

2.1.3 Diagnostic Axes

The ILAE Task Force on Classification and Terminology also proposes a 5-axis (or levels) diagnostic scheme based on (1) ictal phenomenology, (2) seizure type, (3) syndrome, (4) etiology and (5) impairment (ENGEL, 2001). Further, the EEG is recommended for investigation of levels 1, 2, 3 and can be valuable in analysis of axis 4 (ILIESCU *et al.*, 2013).

Meanwhile, non-specific abnormalities do not establish the diagnosis of epilepsy without further investigations. Likewise, a normal EEG does not exclude the epilepsy diagnosis (ENGEL, 2001). Thus, epileptiform discharges are found in 5-8% of normal children EEG. Such findings do not support the diagnosis of epilepsy without seizures or cognitive or language impairment. Likewise, the presence of those symptoms can be correlated to electroclinical syndromes such as Landau-Kleffner syndrome (LKS) (ILIESCU *et al.*, 2013).

Therefore, 0.5% of healthy young adults have incidental epileptiform abnormalities in EEG (SIGN, 2015). Besides, epileptiform abnormalities are found within 29–38% single routine EEG recording of adults who have epilepsy. Furthermore, the sensitivity is improved by recordings repetition (69–77%) and by recording EEG soon after a seizure, during sleep or following sleep deprivation (SIGN, 2015). Accordingly, the prognostic value of epileptic discharges in EEG was related with a risk of seizure recurrence of 83% when performed next a first seizure (VAN DONSELAAR *et al.*, 1992).

2.2 EEG

The electrocortical activity consists of the ionic current generated by biochemical sources, which can be measured in the brain or head surface (NIEDERMEYER and SILVA, 2005). However, the discharge of a single neuron or nerve fiber is not enough to be recorded from the scalp. Thus, it is necessary synchronous cooperation of many neurons, until the sufficient level of extracellular current flow is reached (BUZSÁKI and TRAUB, 2008; GUYTON and HALL, 2006). This neuronal synchrony can occur either by external inputs or by self-generated oscillations. Hence, such current flow can be measured by extracellularly placed microelectrodes, subdural or scalp electrodes (BUZSÁKI and TRAUB, 2008).

Therefore, the Electroencephalogram (EEG) represents the overall activity recorded using pairs of scalp electrodes. Likewise, EEG is described both by foreground patterns (e.g., epileptic spikes) and ongoing background activity (VAN DRONGELEN, 2006). Thus, at routinely clinical EEG, such background activity is classified within different frequency bands (rhythms): delta: 0-4 Hz, theta: 4-8 Hz, alpha: 8-12 Hz, beta: 12-32 Hz and gamma: 32-70 Hz (VAN DRONGELEN, 2006).

Besides, the international standard 10-20 system is commonly used for electrode placement and correlation of external skull locations and cortical areas (VAN DRONGELEN, 2006). Although locations are fixed in this system, the number of used electrodes can vary depending on usage. Hence, fewer electrodes are typically used for neonatal EEG recording due the small size of the head. Thus, in order to avoid record overlapping, usually nine scalp positions are used (MIZRAHI *et al.*, 2004). Examples of electrode placement modified for neonates and standard 10-20 system are shown in Figure 2.1.

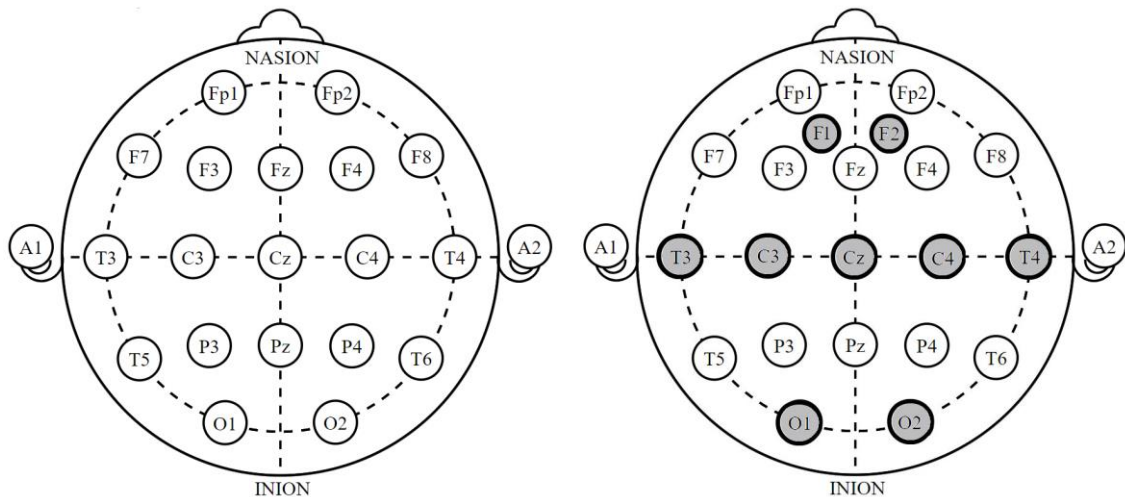


Figure 2.1 – The standard 10-20 system of electrode placement at right. At left, modified for neonates nine scalp positions typically used for neonates were highlighted. Public domain modified.

Although methods as video-EEG are also available for monitoring patients with severe and recurrent seizures, such resources still have limited access and high costs (RENNIE *et al.*, 2004). Hence EEG is a readily available method for diagnosis, classification or characterization of physiologic basis of persons with seizures or epilepsy (PEDLEY, 2008).

2.2.1 Epileptic Activity in Electroencephalography

The presence of epileptic patterns in EEG was first described by Gibbs and colleagues, who demonstrated a 3-per-second spike wave discharge during an epileptic event (GIBBS *et al.*, 1968). Further, albeit many epilepsy syndromes have been associated with specific EEG features, the interictal epileptic discharges (IED) remain characteristic of epilepsy. Such pattern shows cortical hyperexcitability and hypersynchrony. Hence, the IED are strongly correlated with clinical epilepsy, whereas other abnormalities are much less specific (PILAI *et al.*, 2006; SMITH, 2005).

Besides, the presence and frequency of IED in EEG is influenced by factors as age, epilepsy syndrome, seizure types or location of an epileptogenic zone. Thus, children are more likely to present IED than older subjects. Likewise, temporal lobe epilepsy patients are more likely to show IED than those with epileptic foci in mesial or

basal cortical regions, remote from scalp electrodes. In addition, seizure attacks frequency and timing of EEG recordings are also important. Thus, KING and colleagues reported that EEG recordings pursued within 24 hours of a seizure demonstrated more IED (51%) than those recorded later (34%) (KING *et al.*, 1998).

Further, the incidence of IED is considerably low in healthy subjects without history of seizures (0.5% in adults and 2–4% in children). Such incidence is slightly higher for subjects with cerebral pathologies (10–30%). Accordingly, the sensitivity of first EEG recording ranges between 29% and 55%, whereas the sensitivity for repeated recordings varies between 80 and 90% (SALINSKY *et al.*, 1987; ZIVIN *et al.*, 1968). Such wide range may be related to differences in studies methodologies and IED recording requirements (PILAI *et al.*, 2006). Thus, for a description of the criteria needed for a transient to be defined as a specific IED reader is referred to PILLAI and SPERLING (2006).

Accordingly, assessment of IED is often useful for evaluation of epileptic resection region for epilepsy surgery (PILAI *et al.*, 2006). However, the IED has limited use in chronic controlled or resolved epilepsy and localization of extratemporal epilepsies (PILAI *et al.*, 2006; SMITH, 2005). Besides, although the interictal spikes are not always related with seizures, the absence of the IED usually cannot support a negative diagnostic for epilepsy (PILAI *et al.*, 2006).

Moreover, the distinction between ictal (during), interictal (between) and postictal (after a seizure) is not always well delimited. Such transition patterns can be described in terms of rate (abruptly or stuttering), location (seizure ceases simultaneously or not) and seizure intervals (FISCHER *et al.* 2014). Thus, an abrupt interruption of ictal activity and subsequent postictal EEG depression or slowing is seen in scalp recording (SO and BLUME, 2010). Yet, SO and BLUME (2010) reports that such depression is possibly a result of signal attenuation since a clearer termination of ictal period is seen in intracranial recordings.

Furthermore, assessment of the presence or extent of postictal activity depends on location, intensity of the seizure process or epileptic syndrome. Thus, the EEG postictal depression location often can be related with the site of seizure onset in scalp EEG recordings (SO and BLUME, 2010).

2.3 DATA REDUCTION TECHNIQUES

The conventional EEG is described by FELDMAN AND ELLIS (1967 *apud* MAYNARD *et al.*, 1969) with limited use in routine monitoring due to its costs and high skilled operation needs. Thus MAYNARD *et al.* (1969) presents the use of the cerebral function monitor (CFM) to access cerebral activity changes over continuous monitoring from the time-compression, rectification and filtering of the traditional EEG.

Such equipment provided a long-term EEG in a reduced form and less effort to electrodes maintenance. Therefore, the CFM offers the opportunity of reduce the time and cost expenditures due to EEG recording and analyzing processes (HELLSTRÖM-WESTAS *et al.*, 2006).

2.3.1 Amplitude-integrated Electroencephalography (aEEG)

The family of EEG recorders that are designed based on the analogic equipment proposed by MAYNARD *et al.* (1969) is referred by the general phrase CFM. The data reduction method used in the CFM was then called Amplitude-integrated Electroencephalography (aEEG) and the outputs of aEEG recorders are referred as aEEG and aEEG tracing (ZHANG and DING, 2013).

Such method was originally applied to assess brain damage from long-term EEG in order to estimate survival prediction in cardiac arrest adult patients. Further it found also important applications in neonatal medicine to assess perinatal asphyxia outcome (EL-DIB *et al.*, 2009; HELLSTRÖM-WESTAS *et al.*, 2006). Thereafter, ZHANG and DING (2013) proposed a method to calculate a compact aEEG tracing with defined margins using EEG data in order to allow evaluation of this data quantitatively.

However, the use of aEEG also results in loss of detailed evaluation. Nevertheless, it allows to monitor continuously online long-term trends and changes in brain activity (HELLSTRÖM-WESTAS *et al.*, 2006). Therefore, it is also recommend recording of standard EEG, at least once or whenever there is doubt about the aEEG classification (HELLSTRÖM-WESTAS *et al.*, 2006; TOET *et al.*, 2002).

The aEEG signal processing includes pass-band emphasis filtering of 2 to 15 Hz; rectification, envelope obtaining, amplitude compression on a semi-logarithmic scale and time-compression (Figure 2.2) (MAYNARD *et al.*, 1969). Hence, in aEEG brain function monitoring is accomplished by assessment of amplitude trends of brain activity. Thus, lower and upper margins are evaluated by classification methods as they reflect maximum and minimum fluctuations in cerebral activity (ZHANG and DING, 2013).

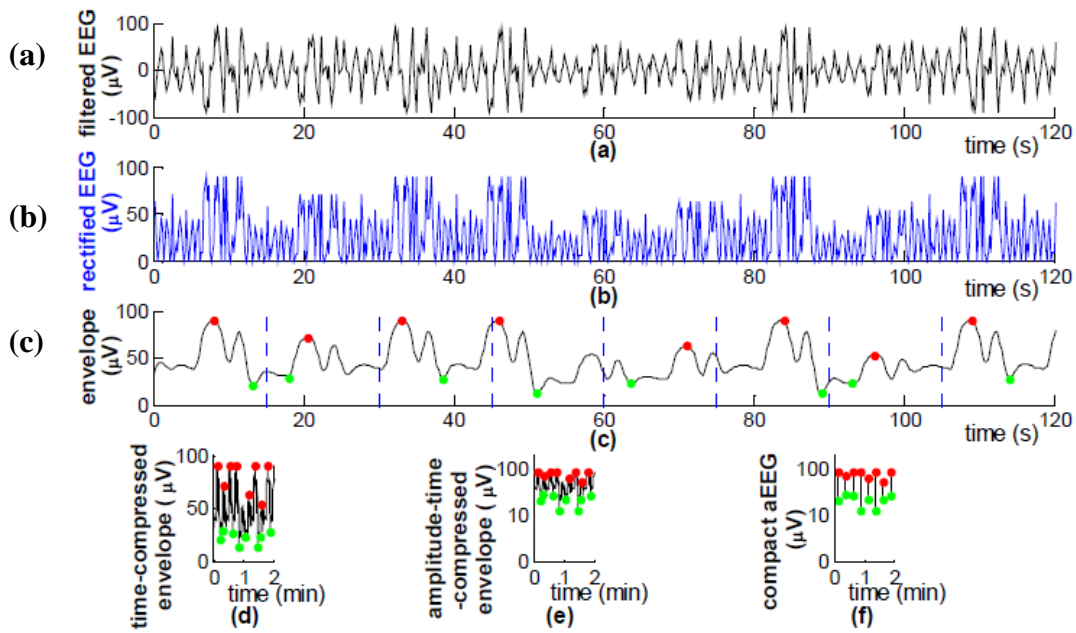


Figure 2.2 – Schematic diagram of aEEG signal processing algorithm. A. Filtered EEG asymmetrically from 2 to 15 Hz; B. rectified EEG signal; C. Rectified signal envelope, with maximum (red) and minimum (green) in each 15-s epoch. D. Time, compressed envelope. E. Amplitude-time compressed envelope F. Compact aEEG tracing. (Adapted from (ZHANG and DING, 2013), under a Creative Commons Attribution license.)

2.3.1.1 Classification and Interpretation of aEEG

The graphical presentation of aEEG is typically accomplished by a display where aEEG tracing is composed of vertical lines representing 15-s of sample data. The highest point of this line shows the maximum amplitude, while the lowest point shows the minimum amplitude. Further, time and amplitude are represented by x-axis and y-axis respectively. Hence, the dense band created over time, which exhibits an activity

trend, is called the activity band (SHAH e WUSTHOFF, 2015; ZHANG and DING, 2013).

Furthermore, the aEEG is frequently used to assess background changes, seizure activity and sleep-wake cycles evaluation. Therefore, dominant pattern of aEEG tracing is the background activity (SHAH and WUSTHOFF, 2015). Such pattern is also affected or depressed by medication effects, arousal, or gestational age (HELLSTRÖM-WESTAS *et al.*, 2008).

Likewise, the interpretation of aEEG background is usually performed by two classification methods: the voltage criterion, proposed by Al Naqeeb *et al.* (1999) and the pattern criterion, proposed by Toet *et al.* (1999) (SHAH and WUSTHOFF, 2015; ZHANG and DING, 2013). Thus, the first method is based only on amplitude of the upper/lower margin values. Meanwhile, the pattern criterion uses defined patterns as characterization feature (ZHANG and DING, 2013).

Moreover, Hellström-Westas (2006) and colleagues acknowledges that, albeit the amplitude of EEG activity is an extremely important measurement, it must be interpreted with caution as voltage may be affected by a variety of factors (HELLSTRÖM-WESTAS *et al.*, 2006). Nevertheless, the use of normative values for minimum and maximum amplitudes of the aEEG within different gestational ages have been helpful to assess neonatal normal development (HELLSTRÖM-WESTAS *et al.*, 2006).

Accordingly, both classification criteria focus on characterization of upper and lower margins of aEEG tracing (ZHANG and DING, 2013). Therefore, summarized information about for available voltage criteria are provided in Table 2.1 and in Table 2.2.

Table 2.1 – aEEG classification according to voltage criterion

Method	Classification	Lower Margin	Upper Margin
Voltage criterion	Normal	> 5 μV	> 10 μV
	Moderately Abnormal	< 5 μV	> 10 μV
	Suppressed	< 5 μV	< 10 μV

Besides, Olischar et al. (2004) categorized aEEG from neonates with no cerebral ultrasonography abnormalities. Thus, 10 minute segments were classified as discontinuous low-voltage pattern (3 μ V to 15-30 μ V), continuous pattern (5 μ V to 20-40 μ V), discontinuous high voltage pattern (3-5 μ V to 20-40 μ V) or bursts (> 100 μ V) (OLISCHAR *et al.*, 2004).

Furthermore, Hellström-Westas et al. (1995) created a classification for asphyxiated term infants as continuous normal voltage (CNV), continuous extremely low-voltage (CLV), burst suppression (BS), and flat (FT). Similarly, Toet et al. (1999) described neonates background patterns during the first six hours of life as continuous normal voltage (CNV), discontinuous normal voltage (DNV), burst-suppression (BS), and flat (mainly isoelectric).

Thereafter, Hellström-Westas (2006) proposed a new classification in order to offer a more general categorization (Table 2.2). Hence, such approach classifies aEEG background pattern of preterm and term infants based on EEG terminology that could be used in all neonates. However, many EEG terms (eg, focal, sharp waves, delta pattern) may not be relevant for aEEG interpretation since this type of information is not provided by such method.

Table 2.2 – aEEG background patterns proposed classification for Preterm and Term Infants based on EEG terminology

Classification	Lower Margin	Upper Margin	Comment
Continuous (C)	> (5-)7-10 μV	< 10–25(–50) μV	Continuous activity
Discontinuous (DC)	< 5 μV	> 10 μV	Discontinuous background
Burst-suppression (BSA)	0-1 μV	> 25 μV	Discontinuous background without minimum amplitude variability
Low voltage (LV)	-	< 5 μV	Continuous background pattern of very low voltage
Inactive, flat (FT)	-	< 5 μV	Isoelectric tracing

A similar voltage criterion was used by TIAN et al. (2012) to evaluate the use of aEEG as a quantitative predictor of outcome in adult patients with Hypoxic Ischemic Encephalopathy (HIE). Such criterion is summarized in table 2.3.

Table 2.3 – aEEG classification according to voltage criterion in adult patients with HIE.

Method	Classification	Lower Margin	Upper Margin
Grade I	Normal	> 5 μV	> 10 μV
Grade II	Moderately Abnormal	\leq 5 μV	> 10 μV
Grade III	Suppressed	> 5 μV	\leq 10 μV
	Mild Abnormality	< 5 μV	< 10 μV

Similarly, the seizure activity in the aEEG is usually identified by a simultaneous and abrupt rise in the minimum and maximum amplitudes (Figure 2.3) (HELLSTRÖM-WESTAS *et al.*, 2006). Such event is often followed by a short post

ictal period of decreased amplitude. Hence, seizures are classified as single seizure, repetitive seizures (single seizures occurring within intervals < 30 minutes) or status epilepticus (seizure activity with duration >30 minutes) (HELLSTRÖM-WESTAS *et al.*, 2006).

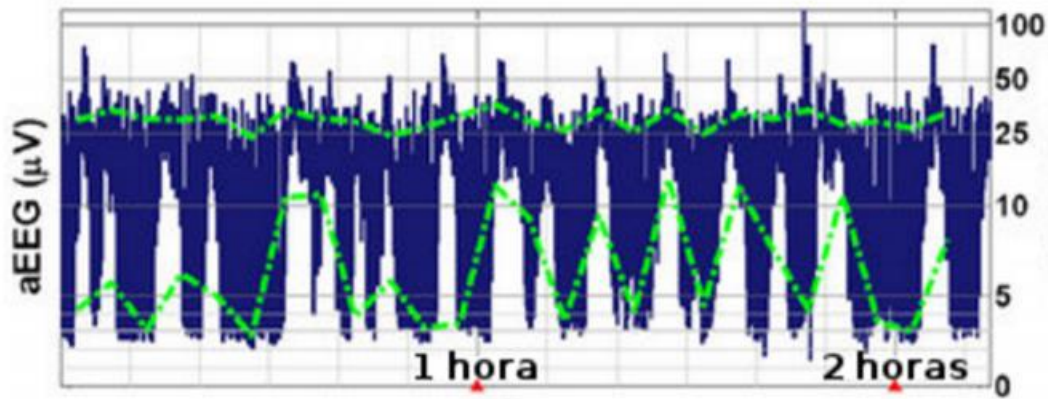


Figure 2.3 – Abnormal aEEG tracings for seizures caused by primary carnitine deficiency in neonate infant (Adapted from (ZHANG and DING, 2013), under a Creative Commons Attribution license).

2.3.1.2 Data acquisition

The commonly used position for electrode placement for the aEEG record has one channel with two symmetric parietal electrodes (P3–P4). Such pair of electrodes were originally recommended by Maynard *et al.* (1969) since those are lesser affected by muscle and ocular movement artifact than frontal and temporal derivations. Further, it also minimizes interference from nursing procedures (HELLSTRÖM-WESTAS *et al.*, 2008).

Furthermore, newer versions of CFM bring use two symmetric pairs of parietals electrodes (C3-P3/C4-P4) as an option (Figure 2.4). Thus, this feature improve identification of focal or asymmetrical electroencephalographic crisis (EL-DIB *et al.*, 2009). Likewise, optionally two frontoparietal bilateral recording channels are also utilized derived from F3–P3 and F4–P4 (HELLSTRÖM-WESTAS *et al.*, 2008).

Nevertheless, since the parietal (P3-P4) electrodes pair is commonly not available on neonatal modified 10-20 system, the (C3-C4) pair is utilized to derive

aEEG from an EEG single channel raw. Such choice is justified by the shorter distance between two pairs of electrodes, which may decrease error chance when using (C3-C4) electrodes pair (SHELLHAAS *et al.*, 2007).

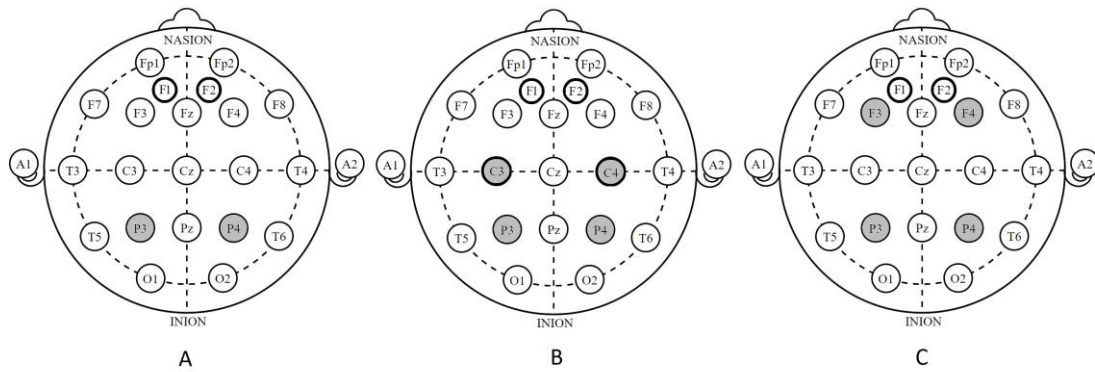


Figure 2.4 – aEEG commonly used electrode placements. A. Parietal electrodes (P3-P4); B. C3-P3 and C4-P4 electrodes. C. Recommended positions for two-channel bilateral recording on neonates (F3–P3/F4–P4).

Besides, more electrodes can be placed to accomplish a multichannel aEEG record (SHAH and WUSTHOFF, 2015). However, in the ICU routine, continuous surveillance or maintenance of impedances and positions of multiple EEG recording set-up is not available (HELLSTRÖM-WESTAS *et al.*, 2008).

Nevertheless, the possibility of measure impedance is important to monitor the state of conductivity of electrodes over long periods (MAYNARD *et al.*, 1969). Thus, continuous monitoring of brain activity with simple recording set-up and montage is required to support clinical decisions in ICU (HELLSTRÖM-WESTAS *et al.*, 2008). Likewise, the analog version of CFM allows continuous monitoring of electrode impedance and contact (MAYNARD *et al.*, 1969).

2.3.1.3 Signal Filtering

The analog implementation of CFM used an asymmetrical filter that allows a greater amplification at higher frequencies. Such filter aims at equalizing the weight of

the energy of rhythmic and nonrhythmic components at each frequency (ZHANG and DING, 2013). Thus this design is justified by the attenuate rate of those latest components, which can achieve 12 dB/dec while transferred through the skull and scalp (MAYNARD *et al.*, 1969).

Further, ZHANG and DING (2013) used a flat band-pass asymmetrical filter acquired with a linear-phase FIR filter designed using the Parks-McClellan algorithm for this purpose. Thus, this filter gave weighted amplification to emphasize alpha frequencies over theta or delta frequencies, while attenuates low-frequency artifacts (EL-DIB *et al.*, 2009; ZHANG and DING, 2013). The schematic diagram of the frequency response of this filter is provided in Figure 2.5.

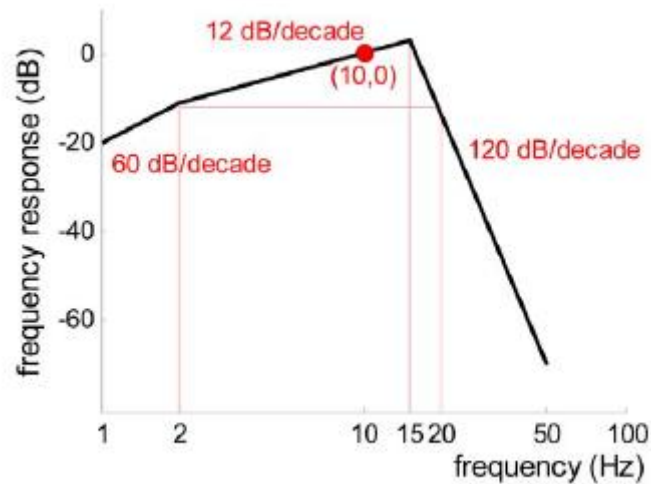


Figure 2.5 – Schematic diagram of the frequency response of the asymmetric filter used in analog CFM (Adapted from (ZHANG and DING, 2013), under a Creative Commons Attribution license).

2.3.1.4 Signal Envelope

The envelope of EEG signal is the carrier of information on tendency of amplitude changes (ZHANG and DING, 2013). Therefore, the envelope extraction achieve concisely representation of the EEG amplitude by a smooth line that approximately connect the peaks of the rectified EEG (Figure 2.2-c) (ZHANG and DING, 2013).

Furthermore, the envelope detection in analogic CFM is performed by low-pass filter acquired from diode and a resistor-capacitor pair with a 0.5-s time constant (HELLSTRÖM-WESTAS *et al.*, 2008; ZHANG and DING, 2013). Thereafter, the digital algorithm, proposed by Zhang and Ding (2013), used a 5-order Butterworth filter to acquire such envelope.

2.3.1.5 Signal Reduction

The tracing compression in CFM is registered with trace of a slow-speed chart recorder (5 cm/hour), displaying maximums and minimums of amplitude as a dense trace over time (MAYNARD *et al.*, 1969; ZHANG and DING, 2013). Then, in the compact algorithm proposed by Zhang *et al.* (2008; 2013) time compression (*x*-axis) is performed by laterally compressing the envelope. Likewise, the amplitude compression is achieved representing the envelope with a base 10 log-scale *y*-axis in order to reduce the dynamical range of large fluctuations in the raw EEG (ZHANG *et al.*, 2008).

Furthermore, most of the information of electrocortical activity is within the pixels on the upper and lower edges of the aEEG tracing. However, due pixels overlap aEEG tracing obtained from compressed envelope aEEG data can be largely reduced for storage and transfer. Such compact tracing is acquired by division of the envelope of rectified signal into non-overlapping epochs of 15-s duration (ZHANG and DING, 2013).

Besides, noise is depressed by picking up the terminal point near (but not at) the upper/lower edge in the algorithm. Such points are defined as the upper terminal position is a percentage near (but lower than) 100% while the lower terminal position is a percentage near (and higher than) 0% (ZHANG and DING, 2013). Thus, percentage unit was used to define position of the selected terminal data in each 15-s epoch sorted and arranged in an ascending order of amplitude (ZHANG and DING, 2013).

Furthermore, using digital algorithm, identification of upper and lower margins of aEEG tracing is performed by connecting lines of the terminal points. Those margins are acquired using the median (not the mean) of every successive 20 terminal points as the upper/lower margin. Indeed, median measure is chosen because its insensitivity to

outliers with extremely high amplitudes since it is noise-proof (ZHANG and DING, 2013).

2.3.2 Hilbert Amplitude-integrated Electroencephalography (HaEEG)

2.3.2.1 Hilbert Transform and analytic signal

The Hilbert Transform (HT), in the Time Domain is a linear operator that produces a real-valued time-domain signal. Such output, $\tilde{x}(t)$ of $x(t)$, is also orthogonal to input function (BENDAT and PIERSOL, 2010). Thus, for continuous signals the HT is defined as an integral by Bendat and Piersol (2010) as:

$$\tilde{x}(t) = H[x(t)] = x(t) * \frac{1}{\pi t} = \int_{-\infty}^{\infty} \frac{x(\tau)}{\pi(t - \tau)} d\tau \quad (2.1)$$

Although the improper integral in the above definition requires the calculation of Cauchy principal value, for discrete signals such operation is not needed. For those signals the integration is represented as a summation (OPPENHEIM and SCHAFFER, 2010).

Furthermore, the HT can also be defined as an Imaginary Part of the Analytic Signal, defined by

$$z(t) = x(t) + j\tilde{x}(t) \quad (2.2)$$

The analytic signal is a complex signal that has no negative frequency components and, hence, it is possible to show the correlation between HT and the analytic signal. Such relation is presented at the Appendix A.

Moreover, the Fourier Transform of a real function is symmetric. Thus, it can be represented as an analytic signal. This definition is useful to determine the amplitude, $A(t)$, and instantaneous phase of a signal, $\theta(t)$, as bellow:

$$A(t) = \sqrt{x^2(t) + \tilde{x}^2(t)} \quad (2.3)$$

$$\theta(t) = \text{arctg} \left[\frac{\tilde{x}(t)}{x(t)} \right] \quad (2.4)$$

Thus, the instantaneous amplitude, $A(t)$, is also referred as the envelope for narrow band signals (BOASHASH, 1992).

Further, the HT can also be defined as a $(\pi/2)$ Phase Shift System. Thus, a FIR Filter phase shift combined with a delay filter can be used for this purpose (BENDAT and PIERSOL, 2010; OPPENHEIM *et al.*, 2010). Accordingly, for detailed treatment of discrete Hilbert Transforms the reader is referred to Oppenheim and Schaffer (2010) and Papoulis (1977).

2.3.2.2 Computation of Hilbert aEEG

The acquisition of a signal envelope can also be performed based on Hilbert Transform as described at 2.3.2.1 (ZHANG and DING, 2013). An adaptation of aEEG method that uses this approach is named Hilbert aEEG (HaEEG) (DE MELO *et al.*, 2014). As previously described for aEEG, the signal processing for HaEEG includes rectification, smoothing and amplitude-integration. However, this method differs from the first on two steps: acquisition of signal envelope and frequency range as discussed further.

Besides, the interpretation of the HaEEG activity is usually accomplished based on commonly used aEEG classification criteria. However, the acquisition of the envelope based on the Discrete Hilbert Transform (DHT) causes a divergence between reference values of voltage classification methods (HELLSTRÖM-WESTAS *et al.*, 2006; OLISCHAR *et al.*, 2004; ZHANG and DING, 2013) and estimated amplitude (DE MELO *et al.*, 2015).

2.3.2.2.1 Signal Filtering

Each derivation is filtered separately within two frequency ranges: the asymmetrical band (2-15 Hz) and the clinical overall band (1-70 Hz). Thus, an IIR multi-band bandpass filter was used for achieve asymmetrical filtering (Figure 2.6) (DE MELO *et al.*, 2014). Further, a pass-band Butterworth filter is also used to perform the clinical band filtering (Figure 2.7) (DE MELO *et al.*, 2014; 2015; DOS SANTOS *et al.*, 2017). Besides, the previously narrower frequency band could hide characteristics of the ictal segment. Hence the evaluation of the overall clinical band frequency intends both delimiting frequency band for HT application and allowing analysis of electrocortical trends within this band (DE MELO *et al.*, 2015).

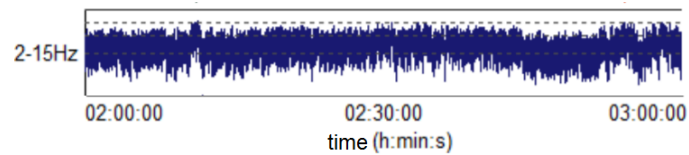


Figure 2.6 – HaEEG for parietal electrodes (P3-P4).for signal filtered at asymmetrical band (2-15 Hz). Adapted from (DE MELO *et al.*, 2014).

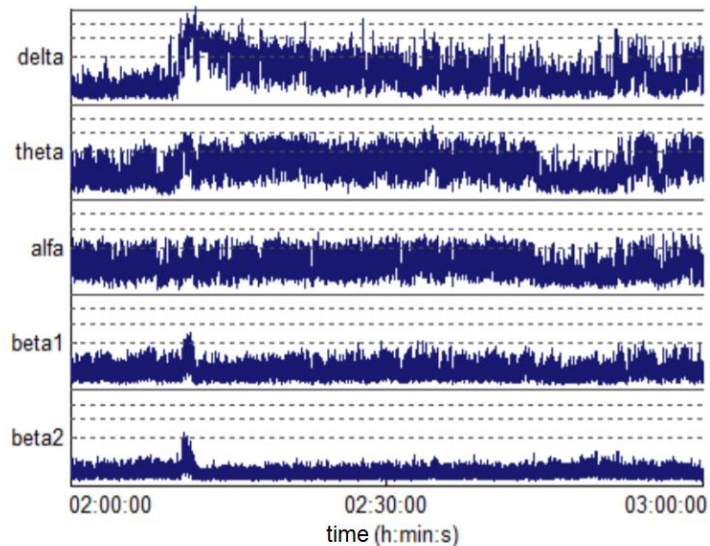


Figure 2.7 – HaEEG for parietal electrodes (P3-P4).for signal filtered at overall clinical band (1-70 Hz). Adapted from (DE MELO *et al.*, 2014).

2.3.2.2.2 Signal Envelope

The analytic signal is acquired based on HT as described at 2.3.2.1. The envelope can then be obtained from the evaluation of the magnitude of the analytic signal (Figure 2.8) (DE MELO *et al.*, 2015).

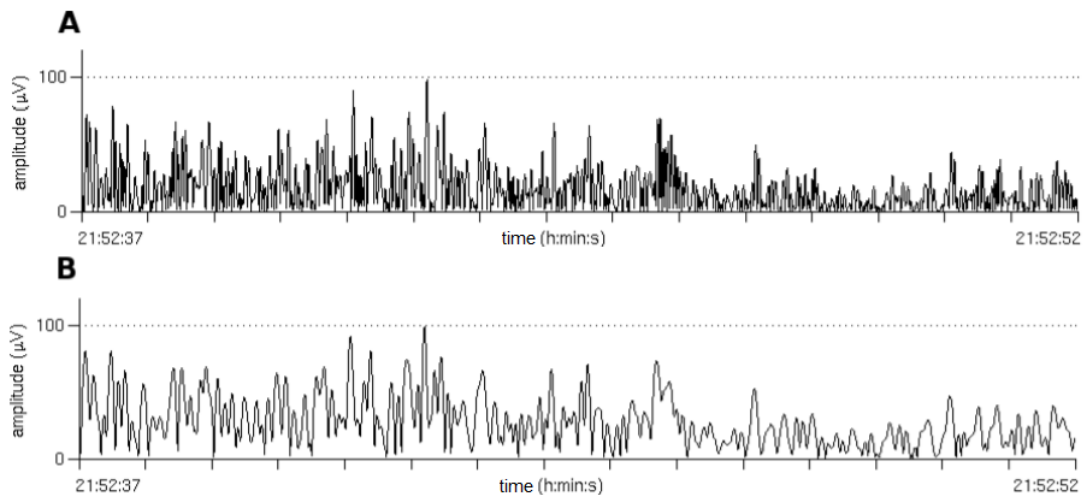


Figure 2.8 – HaEEG envelope acquisition for 15-s ictal segment. A. rectified signal B. envelope acquired from analytic signal using HT (Adapted from de Melo (2015)).

2.3.2.2.3 Signal Reduction

The signal size is reduced (0,16% of original size) by acquisition of 10 and 90 percentiles for each segments (5-s or 15-s) of signal envelope (DE MELO *et al.*, 2014; 2015). Those percentiles were chosen in order to avoid artifacts from extremes values, and thus delimit the superior and inferior limits of reduced envelope (DE MELO *et al.*, 2015).

Those limits are display as a dense trace of vertical lines over time. Therefore, at the graphical display the *x*-axis and *y*-axis respectively represents time and EEG amplitude. Thus, *y*-axis is represented both on a linear scale (0 a 10 µV) and on a logarithmic scale (10 a 100 µV) (DE MELO *et al.*, 2014).

2.3.2.3 Instantaneous Frequency Estimation

The instantaneous frequency (IF) can also be acquired from the analytical signal and is defined by Bendat and Piersol (2010) as:

$$\omega(t) = \frac{d\theta(t)}{dx} \quad (2.1)$$

expressed in radians per second (rad/s) or

$$F(t) = \frac{1}{2\pi} \frac{d\theta(t)}{dx} \quad (2.2)$$

expressed in Hertz (Hz).

Further, according to the definition presented above, only one frequency component exists for each instant. However, a divergence arises from this concept since there are authors who suggest that its physical meaning only exists for monocomponent signals (HUANG *et al.*, 1998). This type of signal is described as those that present only positive values of instantaneous frequency (HUANG *et al.*, 1998).

Besides, a narrow range of frequencies varying as a function of time is enough condition for the definition of a monocomponent signal. A more detailed discussion of controversy in defining instantaneous frequency (IF) can be found at in Huang *et al.* (1998).

Therefore, the use of Huang-Hilbert Transform (HUANG *et al.*, 1998) and Hilbert vibration decomposition (FELDMAN, 2006) were proposed to decompose the signal into components for which the IF can be defined. However, this latest method is restricted for periodic and quasi-periodic signals. Hence, Freeman (2007) proposed the clinical mode decomposition method, which uses a pass-band filter to decompose signals within the clinical spectrum.

Accordingly, the definition of HT from the analytic signal allows implementation of Discrete Hilbert Transform (DHT) based on Fast Fourier Transform (FFT) (MARPLE, 1999). Thus, for a signal with an even number of elements:

$$Z[k] = \begin{cases} X[k], k = 0 \text{ and } k = \frac{N}{2} \\ 2X[k], 1 \leq k \leq \frac{N}{2} - 1 \\ 0, \frac{N}{2} + 1 \leq k \leq N - 1 \end{cases} \quad (2.3)$$

whilst, similarly, for an odd number of elements:

$$Z[k] = \begin{cases} X[k], k = 0 \\ 2X[k], 1 \leq k \leq \frac{N-1}{2} \\ 0, \frac{N+1}{2} \leq k \leq N-1 \end{cases} \quad (2.4)$$

The transform terms of $X[0]$ and Nyquist frequency $X\left[\frac{N}{2}\right]$, are shared between positive and negative frequency spectrum. Hence, those points are not multiplied by two and the energy is shared between the two sides of the spectrum (MARPLE, 1999).

Accordingly, for discrete signals amplitude ($A[n]$) and frequency ($F[n]$) are defined by Long (2004) as:

$$A[n] = \sqrt{x^2[n] + \tilde{x}^2[n]} \quad (2.5)$$

$$F[n] = \frac{\tilde{x}'[n]x[n] + \tilde{x}[n]x'[n]}{x[n] + \tilde{x}^2[n]} \quad (2.6)$$

where $\tilde{x}'[n]$ and $\tilde{x}[n]$ are the first derivative acquired from numerical methods

$$x'[n] = \frac{x[n+1] - x[n]}{T_s} \quad (2.7)$$

$$\tilde{x}'[n] = \frac{\tilde{x}[n+1] - \tilde{x}[n]}{T_s} \quad (2.8)$$

respectively, where T_s is the sampling period.

2.4 PERFORMANCE METRICS

2.4.1 Accuracy, Sensibility and Specificity

The performance of a classification method can be evaluated using the cross tabulation between the model predicted class and the actual sampled class. This tabulation is known as the contingency table (Table 2.3) (also called the confusion matrix) (PRATI *et al.*, 2008).

Therefore, a binary classifier can be described in two classes: positive and negative. Thus, for a given positive sample, it can be either correctly identified as True Positive (TP) or as incorrectly classified as a False Negative (FN). Similarly, negative samples can be classified as False Positives (FN) or True Negatives (TN). Thus, the confusion matrix presents the occurrence count of those classes for a given classifier along with the amount of positives predictions (PP), negative predictions (NP), actual positives (POS), actual negatives (NEG) and the number of sample elements (N) (PRATI *et al.*, 2008).

Table 2.3 – Confusion matrix for a binary classifier

		Predicted		
		Yes	No	
Actual	Yes	TP	FN	POS
	No	FP	TN	NEG
		PP	NP	N

Furthermore, a classification method performance can also be statistically measured by computing classification accuracy (Acc), sensitivity (Sen) and specificity (Spe) based on contingency matrix entrances as defined bellow

$$Acc = \frac{TP + TN}{TP + TN + FP + FN} \times 100$$

$$Sen = \frac{TP}{TP + FN} \times 100 \tag{2.9}$$

$$Spe = \frac{TN}{TN + FP} \times 100$$

2.4.2 ROC Curve

The ROC (Receiver-Operating Characteristic) curve is a method for evaluating the accuracy of a test with output within an ordered range of values. This analysis is performed by defining a classification threshold beyond which values are classified as positive or negative. The ROC Curve is achieved by 2-D line plotting of true positive rate (Sensitivity) at y-axis the false positive rate (1-Specificity) at x-axis for different decision threshold points. Further, optimal decision threshold is the one that maximizes

the Sensitivity/Specificity ratio which can be obtained from the ROC curve (ZWEIG and CAMPBELL, 1993).

Therefore, for the normalized point $(1 - \text{Spe}, \text{Sen})$, the value of the Area Under the ROC Curve (AUC) also vary between 1 and 0. Such area can then be used to evaluate the classifier performance: the closer AUC is to 1, the higher the accuracy of the test. Accordingly, AUC value near to 0.5 indicates a classifier that operates at chance level. Likewise, a common evaluation of the ROC curve uses the accuracy value (ZWEIG and CAMPBELL, 1993).

Furthermore, correlated ROC curves (based on tests performed on the same individuals) can be evaluated using the Delong method. Such method is a nonparametric approach for the analysis of the AUC, by generating an estimated covariance matrix (DELONG et al., 1988). Thus, the confidence interval of the difference between paired AUCs can be obtained from such estimated covariance matrix (HANLEY e HAJIAN-TILAKI, 1997).

2.5 EEG DATA INTEGRATION PLATFORM

2.5.1.1 Platform Design

The integration and processing of EEG data from multiples sources poses different challenges. Accordingly, different needs and structures of each partner pose individual requirements for EEG system setups. Besides, it may be required to processes and transfer a large amount of data between integration sites (IHLE *et al.*, 2012).

Therefore, for the European EPILEPSIAE database project, IHLE and colleagues argues that a distributed architecture offers easier administration and lighter network traffic whereas replicated databases offer advantages regarding data access and security (IHLE *et al.*, 2012). Although a replicated architecture was chosen, the project reports that, later, a distributed database may be required for handling the increasing data volume. However, such solution could be very demanding for the network infrastructure (IHLE *et al.*, 2012).

In addition, Beniczky and colleagues reports that the standardization of EEG reports and finding could also potentially help to integrate computer-assisted analysis into the report and development an international standardized database (BENICZKY *et al.*, 2013).

Besides, along with a relational database, an EEG integration system need also provide a user-friendly way for the systematical access of datasets from the database without expert knowledge of database schema or SQL (Structured Query Language) (IHLE *et al.*, 2012).

2.5.1.2 EEG Recordings Metadata

The EEG management file systems must contain patient metadata information such as name, birth date, medical history and EEG files saved on that patient. Likewise, each EEG file should carrier information of electrode placement, computer, amplifier and filtering settings and hospital unit number or name, recording date and name or initials of the technologist (HALFORD *et al.*, 2016; LESSER and WEBBER, 2005; SINHA *et al.*, 2006).

Besides, the American Clinical Neurophysiology Society (ACNS) recommends that clinical EEG records includes patient last seizure date (when know), testing time stamp and the behavioral state of the patient. Therefore, information about the recording protocol and patient overall state (*e.g.* premedication given, awake state) may also be helpful (SINHA *et al.*, 2006).

Similarly, an annotation file must provide log information of the times and locations of EEG items that have been identified with seizure events, along with descriptive information by reviewer (LESSER and WEBBER, 2005). Furthermore, LESSER and WEBBER (2005) suggest that this file should be unique for each patient. In contrast, publicly available EEG databases, such as CHB-MIT Scalp EEG Database, often provide separate annotation files (GOLDBERGER *et al.*, 2000; SHOEB and GUTTAG, 2009). Accordingly, ACNS recommends that EEG recording formats stores technologist's comments and event codes within the EEG signal data (HALFORD *et al.*, 2016). Further, such clinical metadata information may allow the use of machine

learning algorithms to evaluate clinical practices and diagnostics (OBEID and PICONE, 2016).

3 LITERATURE REVIEW

3.1 DATA ANALYSIS AND SEIZURE DETECTION

The ability to detect or predict clinical seizures can allow tailored therapies, prevent accident (injuries) or SUDEP (Sudden Unexpected (or Unexplained) Death in Epilepsy). Indeed, albeit newer antiepileptic drugs have been introduced, nearly one-third of epileptic patients continue to have seizures despite optimal medication management. Thus, for this group a prediction-based treatment could change continuous treatment to timely targeted medical interventions (IHLE *et al.*, 2012). Therefore, several algorithms were proposed to computation and classification of EEG features in automated seizure detection and prediction (RAMGOPAL *et al.*, 2014).

Automated seizure detection algorithms aim to determine the presence or absence of ongoing seizures. Accordingly, such systems involve two main steps: computation and classification. Thus, required EEG features and quantitative values must be acquired from the data. Further, classification criteria must be applied to determine the presence or absence of a seizure. (RAMGOPAL *et al.*, 2014).

Therefore, a detection algorithm for the automatic screening of electrographic neonatal seizures in aEEG signals was proposed by LOMMEN *et al.* (2007). Such method considered a sudden increase of the lower boundary as pattern of interest. Thus, this study evaluated 13 recordings and achieved sensitivity $\geq 90\%$ for 5 of than with approximately 1 false positive per hour. In addition, LOMMEN *et al.* (2007) reported that the algorithm presented much lower sensitivities for an extremely high amplitude recording that were incorrectly classified as artifact or recordings with poor interobserver agreement (LOMMEN *et al.*, 2007).

However, SHELLHAAS (2007) reported a poor aEEG sensitivity for neonatal seizure detection by neonatologists when using aEEG notably when events are infrequent, brief, or of low amplitude (SHELLHAAS *et al.*, 2007). Further, the diagnostic use of aEEG for the detection of seizures in adult patients for the identification of epileptic seizures in the hands of nonexpert ICU physicians was reported with a mean sensitivity 40% (NITZSCHKE *et al.*, 2011). Thus, those studies

report the use of the aEEG as supplemental resource but not as a replacement for conventional EEG (NITZSCHKE *et al.*, 2011; SHELLHAAS *et al.*, 2007).

Meanwhile, several studies intended to evaluate the clinical value of aEEG for prediction short-term neurological outcome in term and preterm newborns at risk of neurologic injury (AL NAQEEB *et al.*, 1999; BOUREZ-SWART *et al.*, 2009; EVANS *et al.*, 2010; LAERHOVEN *et al.*, 2013). Nonetheless, despite the aEEG has been established as a selection criterion for hypothermic neuroprotection for neonates, Sarkar and colleagues reported that the aEEG should not be used as the only selection criterion for this propose. Such study showed early death or MRI findings for up to 30% of neonates with normal aEEG tracings (non-qualifying for hypothermia) but clinical signs of encephalopathy. This research also presented a poor correlation (sensitivity of 54.8% and negative predictive value (NPV) of 44%) between early aEEG and short-term outcome for this scenario (SAKAR *et al.*, 2008).

Besides, some CFM machines also offer other trends than the aEEG, including density spectral array (DSA) which could be helpful to detect seizures (HELLSTRÖM-WESTAS, *et al.*, 2008). Accordingly, STEWART *et al.*, (2010) reported a median sensitivity for seizure detection of 83.3% using CDSA (color DSA) and 81.5% using aEEG across 27 ICU recordings. In addition, the study highlighted low-amplitude, short and focal seizures as a sensitivity reducing factor (STEWART *et al.*, 2010).

Similarly, Hilbert Transform (HT) analysis can also give additional important information of signal components thorough instantaneous frequency estimation. Therefore, WITTE *et al.* (1991) evaluated the use of Discrete Hilbert Transform (DHT) during automatic spike mapping. Such study reported that occurrence of epileptic spikes are characterized by a higher envelope magnitudes and low variance of the instantaneous frequency. However, the application of the DHT produces a reliable estimation only for narrowband signals (WITTE *et al.*, 1991). Hence, HOFFMAN *et al.* (1996) used the HT to compute the spatial distribution of instantaneous power during the occurrence of rolandic spikes. Such feature was used in a Neural Network (NN) classification model for topographically different spike types with sensitivity for spikes from unknown patients of 98%. HOFFMANN *et al.*, 1996).

Furthermore, the Spectral edge frequency (SEF), defined as the frequency below which a given amount of the total EEG power resides, can also give resourceful information on the quality of the electrocortical background activity (HELLSTRÖM-WESTAS *et al.*, 2008). Therefore, KOBAYASHI *et al.* (2011) intended to incorporate SEF information into aEEG figures. Thus, SEF was determined using a percentage of 90% and aEEG tracing was devised into a color scale indicating the SEF of the corresponding time point with a frequency range from 1 to 20 Hz (KOBAYASHI *et al.*, 2011). Such study performed the envelope extraction using the HT for 1 or 15-s data segments. Accordingly, for each patient, each seizure was paired with an interictal period. Further, test reviewers were instructed on how to interpret the figures displaying compressed data in aEEG, DSA, or aEEG/SEF form. Hence, the study reported a median number of correctly identified seizures, within a total of 12, of 7 for aEEG, 8 for DSA and 10 for aEEG/SEF figures (KOBAYASHI *et al.*, 2011). Besides, HELLSTRÖM-WESTAS *et al.* (2008) also reports that SEF can be useful in experimental and clinical studies of white matter injury in preterm infants.

Thereafter, the use of HT to acquire the signal envelope during aEEG digital algorithm was used by DE MELO *et al.* (2014). Besides, a comparison between aEEG asymmetrical filtering (2-15 Hz) and overall clinical bands filtering was investigated. This method, named as HaEEG, used the 10 and 90 percentiles obtained for each 5-s reduced segment (DE MELO *et al.*, 2014). Such study reported higher amplitudes at delta and beta bands during epileptic events for recordings of one subject with mesial temporal lobe epilepsy.

Further, DE MELO *et al.* (2015) reported that HaEEG allowed greater highlighting of electrographic seizures than aEEG. In addition, the clinical bands filtering produces a sensibility-specificity increase for seizure identification and allowed subject and type specific seizure pattern identification. Accordingly, DOS SANTOS *et al.* (2017) evaluated the parameters of envelope acquisition for HaEEG and aEEG. Such study proposed the acquisition of aEEG envelope using a 2nd order Butterworth filter using Square Law without Gain. Moreover, the Hilbert envelope was described as more reliable for signal resembling and seizure highlighting in relation to background activity when compared to Butterworth. Nonetheless, all three studies consistently reported epileptic events were better distinguished within the clinical bands when compared to

the asymmetrical band from 2 to 15 Hz (DE MELO, 2014; 2015; DOS SANTOS et al., 2017).

3.2 EEG DATA INTEGRATION PLATFORM

The need of comprehensive EEG data analysis has led to integration efforts in order to provide high quality data for research purposes. Thus, several centers have reported coordinated efforts to integrate detection and prediction algorithms to suitable EEG data.

Further, the Standardized Computer-based Organized Reporting of EEG (SCORE) software for EEG assessment and reporting was proposed by an ILAE workgroup. Such software intended to standardize EEG assessment and reporting. Thus, this application registers patient personal data, recording conditions and diagnostic suitable data. Accordingly, Beniczky and colleagues report that the SCORE could be used for integration of computer-assisted analysis into the report and development of multinational database, or for teaching purposes (BENICZKY *et al.*, 2013).

Besides, the European project Evolving Platform for Improving the Living Expectations of Patients Suffering from IctAI Events (EPILEPSIAE) released the EPILAB software for the design and evaluation of seizure prediction algorithms (TEIXEIRA *et al.*, 2011). This project also presented an epilepsy database aiming at the development of seizure prediction algorithms. Such database includes extensive information about clinical data in order to contribute specially to epilepsy research. Besides, the database also integrates previously computed features from analytic algorithms in order to enhance process capability and combination of different feature algorithms (IHLE *et al.*, 2012).

Furthermore, the Neural Engineering Data Consortium (NEDC) released the Temple University Hospital EEG Corpus (TUH) which consist of over 25,000 EEG studies, including neurologist's interpretation of the test, a patient information (HARATI *et al.*, 2014). Further, the study reported that an experiment on a subset corpus of 3,762 sessions achieve event prediction directly from the data using unsupervised and partially supervised learning approaches. Thus, this study presented a detection rate of 76% with a false alarm rate of 12% when detecting spike or sharp

waves, Generalized Periodic Epileptiform Discharges and Periodic Lateralized Epileptiform Discharges events with a HMM-based system (HARATI *et al.*, 2014).

3.2.1 Electroencephalogram Database

The evaluation, standardization and reproducibility of seizure prediction studies requires access to high quality long-term EEG data (IHLE *et al.*, 2012). Thus, the management and interoperability of this data depend upon databases that can be used for cross validation of prediction methods. Therefore, this demand motivated the publication of EEG research dataset collections by seizure prediction community (Table 3.1).

Besides, clinical data can be difficult and expensive to obtain for research groups with no direct access to treatment centers (IHLE *et al.*, 2012). Thus, prediction and detection methods based on EEG signal processing continuously face the issue of training pattern recognition engines on small datasets, achieving limited results (OBEID and PICONE, 2016). However, the great variability of the EEG signal requires a suitable amount of data to support evaluation of statistical models of the brain signals (ALOTAIBY *et al.*, 2014; RAMGOPAL *et al.*, 2014).

Accordingly, in Europe, the Bonn EEG database (ANDRZEJAK *et al.*, 2001) hosts continuous intracranial recordings. Similarly, the Freiburg EEG database (WINTERHALDER *et al.*, 2003) contains invasive long-term EEG recordings collected at the Epilepsy Center of the University Hospital of Freiburg in Germany. Moreover, this project also provides pre-ictal (at least 50 min) and interictal data (at least 24 h of non-seizure EEG recordings) for each ictal event.

Further, the EPILEPSIAE project (IHLE *et al.*, 2012) presented the European Epilepsy database hosting long-term continuous EEG data, enriched with clinical metadata as a joint effort of epilepsy centers in Portugal (Coimbra), France (Paris) and Germany (Freiburg). Hence, the previously Freiburg database was superseded by EPILEPSIAE and is no longer available for access.

Similarly, the Australian EEG Database is a web-based de-identified searchable database recorded at a regional public hospital. Conversely, the use of this data depends on research committee approval and access fee payment (HUNTER *et al.*, 2005).

Likewise, the TUH-EEG Corpus is a big data corpus, which consists of EEG studies along with neurologist's interpretation of the tests and demographic information of the patients (HARATI *et al.*, 2014). Further, the Canadian Epilepsy Database and Registry (CEDAR) is a multicenter epilepsy database that allows registered users to enter data for epilepsy research (MCLACHLAN, 1998). Besides, the Flint Hills Scientific, L.L.C., Public ECoG Database (FHS Database) maintains continuous intracranial recordings along with metadata about the seizures events and electrode location (WINTERHALDER *et al.*, 2003).

The publication of public available neonatal dataset collections is also increasing. Although these data sets are not epilepsy specific, such data may be helpful to evaluate automated prognostic and diagnostic algorithms for this age range.

Meanwhile, despite of many independent patient-specific data sets collected within EEG researches, Brazil does not have an open source EEG Database for evaluation of prediction and detection methods.

Furthermore, those databases can be either open access efforts like Bonn EEG Dataset or restrictive licensed sources as EPILEPSIAE and the Australian EEG Database which access requires license purchase. Besides, multi-purpose data repositories as Physionet (GOLDBERGER *et al.*, 2000) are also available. Such repository hosts databases as CHB-MIT Scalp EEG Database (SHOEB and GUTTAG, 2009), which consists of EEG recordings from 22 pediatric subjects with intractable seizures from the Children's Hospital Boston.

Although those efforts, the lack of open source long-term continuous recordings still an issue. Indeed, the limited information on clinical metadata and annotations correlated with the available EEG data represents a drawback for evaluation of detection and prediction algorithms (IHLE *et al.*, 2012). Meanwhile, albeit the large amount of EEG exams performed annually worldwide, little or none of this data becomes available for research. Such amount of clinical data can contribute with more parameters such as electrode montage, clinical environment, equipment, and noise. Therefore, computing this variability can lead to the development of robust, high performance health care technologies (OBEID and PICONE, 2016).

Table 3.1 – EEG data collections for epilepsy available research per region

Region	Database	Data set			Electrode Type
		Subjects	Age range	Records	
North America	CHB-MIT Database	22	Pediatric	664 records, 129 files with 198 seizures	Scalp EEG
	THU EEG Corpus	> 14000	Adult and Pediatric	20,000 clinical EEG records from TUH	Scalp EEG
	CEDAR	> 8000	Adult and Pediatric	8000 recordings from 20 centres	non specified
	FHS Database	10	Adult and Pediatric	1419 h of continuous iEEG recordings at 249 Hz	iEEG
Europe	Freiburg Database	21	Adult and Pediatric	582 hours of intracranial recording, with 88 seizures.	Scalp and iEEG
	Bonn EEG Database	5	non specified	Discontinuous datasets with 40 min of EEG each	iEEG
	EPILEPSIAE	275	Adult and Pediatric	225 scalp, 50 intracranial recordings	Scalp and iEEG
Oceania	Australian EEG Database	18500	Adult Pediatric Neonatal	18500 EEG recordings from John Hunter hospital	Scalp EEG

4 MATERIALS AND METHODS

4.1 CASUISTRY

The EEG data used in the present work is part of the “CHB-MIT Scalp Database” publicly available by Physionet Service (GOLDBERGER *et al.*, 2000). The pediatric age (0-21) was identified as described by the American Academy of Pediatrics (HARDIN *et al.*, 2017). Therefore, those signals consist of EEG recordings from 21 pediatric subjects (4 males and 17 females) with average age of 8.375 years (1.5-19 range) for females and of 9.67 years (3-16 range) for males. Thus, 621 records are available and 125 of those files have seizures previously identified in each record (SHOEB and GUTTAG, 2009; GOLDBERGER *et al.*, 2000).

These records were sampled at 256 Hz with 16-bit resolution. The data is stored in European Data Format (EDF) format and contains between one and four hours of digitized EEG signals per file. In addition, for files that contain one or more seizure, an annotation file is also available with beginning and ending times of each seizure. Thus, records can be divided into non-seizure records – those do not contain seizures – and seizures records – those that contain one or more ictal epochs. The International 10-20 system of EEG was used for these recordings and additional information about the bipolar montage used for each recording is given in Appendix B. Summarized information about patient per each case is also provided in Appendix C (SHOEB and GUTTAG, 2009).

The available signal collection has selected fields, such as protected health information (PHI), previously modified from original signal header in order to ensure patient anonymity (GOLDBERGER *et al.*, 2000; SHOEB and GUTTAG, 2009).

4.1.1 EEG Data

The CHB MIT EEG raw data presents aliasing of harmonics of 60 Hz mains interference as a result of 256 Hz frequency sampling, resulting in frequencies that are multiples of 16 Hz (16 Hz, 32 Hz and 48 Hz). Therefore, a second-order IIR notch digital filter was designed for each of those frequencies (Figure 4.1).

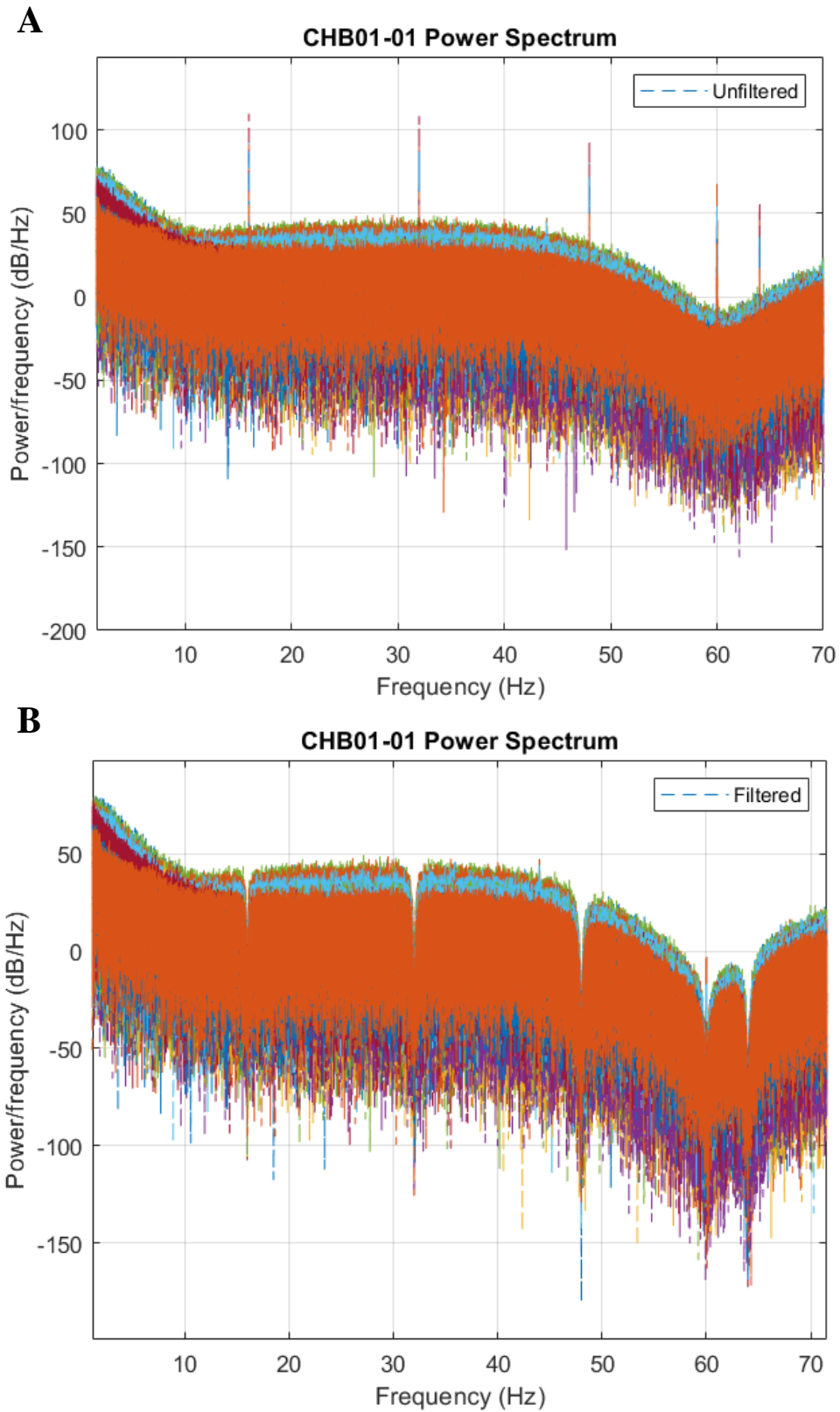


Figure 4.1 – Power Spectral Density of 1 hour of a non-seizure record for subject chb01 A. EEG raw data B. signal filtered at multiples of 16 Hz and 60 Hz.

4.2 INTEGRATION AND PRE-PROCESSING DATA

4.2.1 Data Processing and Orchestration

In order to acquire the EEG raw data from participant centers a TCP/IP solution was proposed. Further, once at the research center accountable for the signal processing, the EEG raw data, recording, channel and patient information are extracted from EEG signal and stored at EEG database. For each patient, the EEG raw data and the extracted metadata are anonymized and became available for research. Likewise, signal and patient de-identified metadata is also generated and made available.

Then, in order to promote data interoperability, the native recordings file formats are converted to EDF format. Nevertheless, the native format remains available, so the processed data keep the backward compatibility with the original center. Therefore, for each patient EEG raw data, two files formats became available after processing. The integration process is shown at Figure 4.2.

Next, the preprocessed EEG data becomes available for the signal processing step and subsequent feature extraction. The signal processing step is further discussed at section 4.3. Such features are stored at the database in order to allow combination of different feature algorithms decrease computation time.

Besides, throughout the process an orchestration service connects the steps of the information flow. This service verifies the files process pipeline and control the transfers file flow between sites.

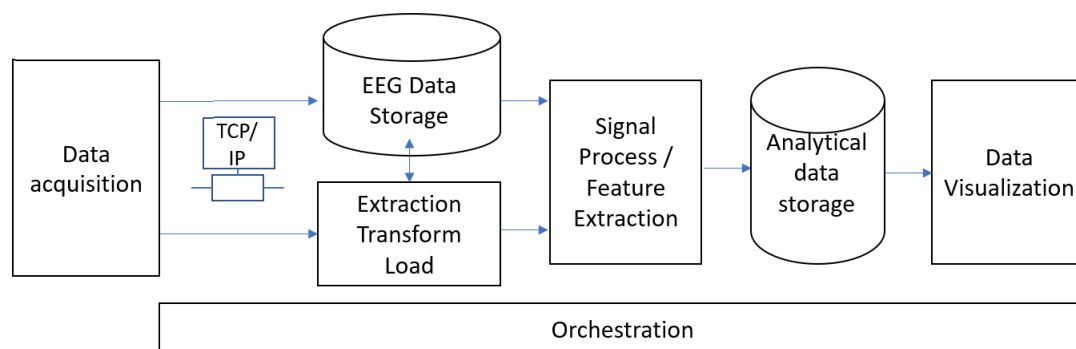


Figure 4.2 – Data integration architecture.

4.2.2 Electroencephalogram database

A centralized database was designed to storage and management the EEG data and the processed features. The database was designed and created using the Microsoft SQL Server 2017 (Microsoft® 2017) which implements relational tables and functions for structured accessing and changing data. Then, SQL Server Management Studio (Microsoft® 2017) was used to administer and design the database in SQL Server.

4.2.3 Client application

A client application for the database designed in this study is provided in order to allow data input, browsing and querying the available the dataset. Such desktop application was developed using the Windows Presentation Foundation (WPF) presentation framework.

The database application can be centrally installed and maintained. Thereafter, development of a web-based application is previewed. In either case, login authentication to the application is required.

4.3 EEG SIGNAL PROCESSING

4.3.1 Filtering Data

The acquired signal was filtered separately within two frequency bands: the asymmetrical band (2-15 Hz) and the clinical overall band (1-70 Hz). Thus, the asymmetrical filter proposed by MAYNARD (1969) was designed using a IIR band-pass filter with an asymmetrical gain and a slope of 60 dB/dec within 0-2 Hz, 12 dB/dec within 2-15 Hz, and -120 dB/dec beyond 15 Hz, with a peak frequency of 15 Hz (ZHANG and DING, 2013). Such filter has similar frequency features to the analog filter used in the CFM as shown in Figure 4.3, which compares the frequency responses of those filters.

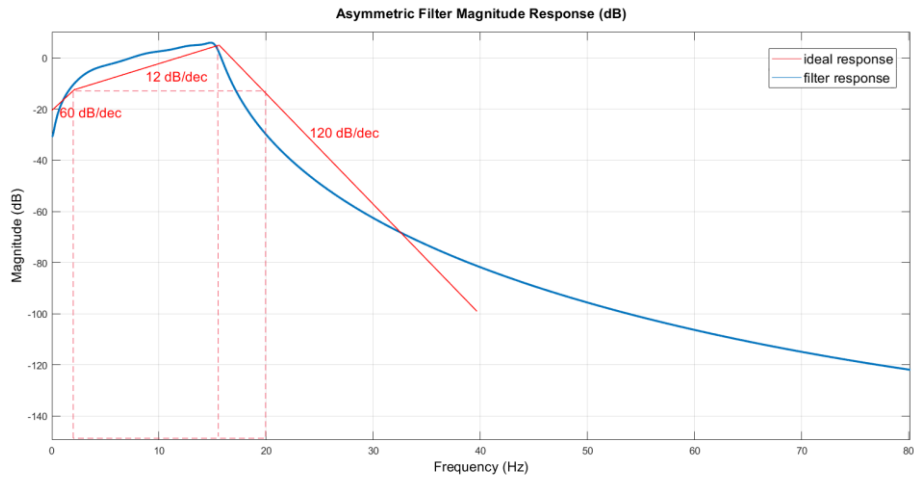


Figure 4.3 – Frequency response for aEEG asymmetric filter

Further, the overall clinical filter was designed as a 20th-order Butterworth bandpass filter. Therefore, this filtering limits the bandwidth of HT and allows trend analysis in each band within electroencephalographic events.

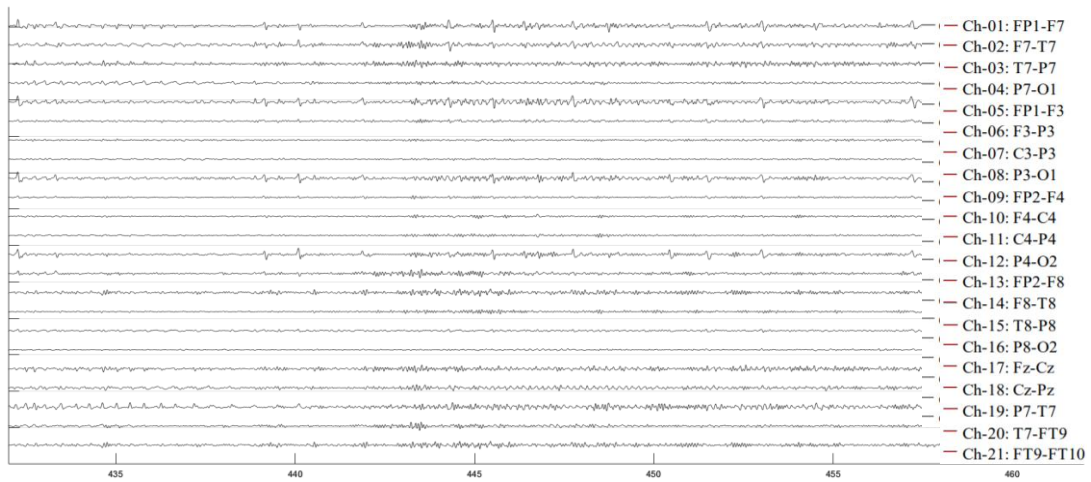


Figure 4.4 – Example of 30s seizure epoch for chb03 subject filtered from 2 to 15 Hz.

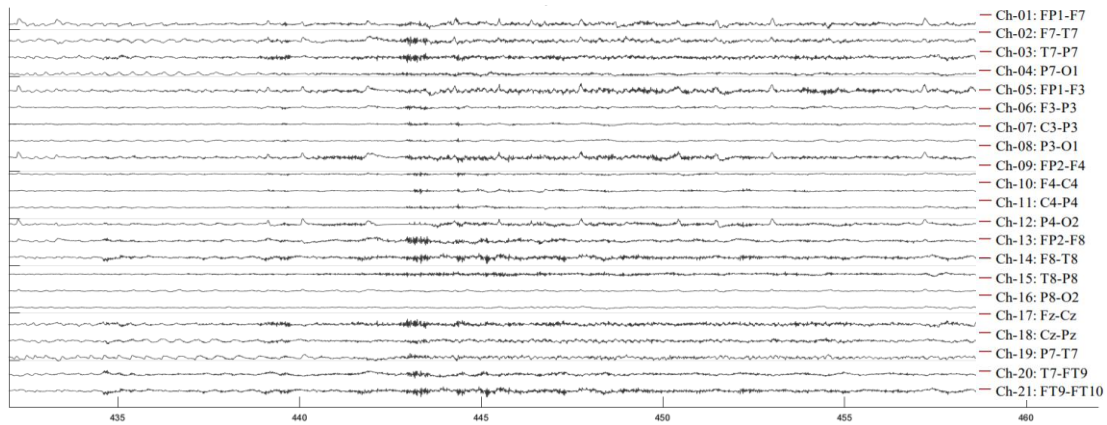


Figure 4.5 – Example of 30s seizure epoch for chb03 subject filtered from 1 to 70 Hz.

4.3.2 Envelope Extraction

The envelope detection was performed both by the CFM analogical filtering and using de Hilbert Transform (Figure 4.6). Thus, the aEEG filter was acquired with a 2nd-order Butterworth filter with a cutoff frequency of 0.3183 Hz (Figure 4.7) which is equivalent to the 0.5-s time constant used in the CFM classical envelope detection performed using a diode and a resistor-capacitor (ZHANG and DING, 2013). The use of order 2 aims to decrease the noise introduced by the oscillatory response of the 5th-order filter used in the digital aEEG (DOS SANTOS et al., 2017).

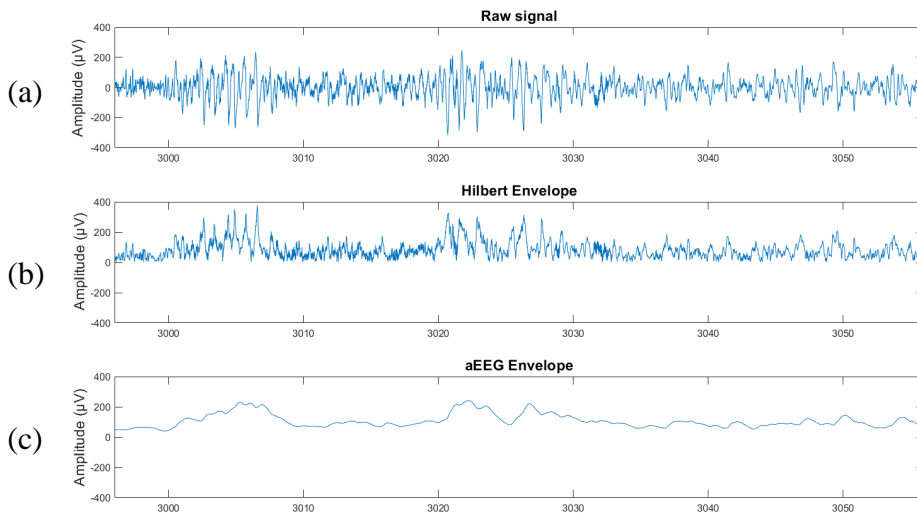


Figure 4.6 – Envelope detection for 15-s seizure epoch of chb03 subject for C3-P3 derivation: (a) signal filtered from 2 to 15 Hz (b) envelope acquisition through low-pass filtering (c) envelope detection acquired from Hilbert Transform and analytic signal.

Further, the envelope extraction was obtained using the magnitude of the analytic signal (Equation 2.5 and 2.2) computed by Hilbert Transform (Equation 2.1).

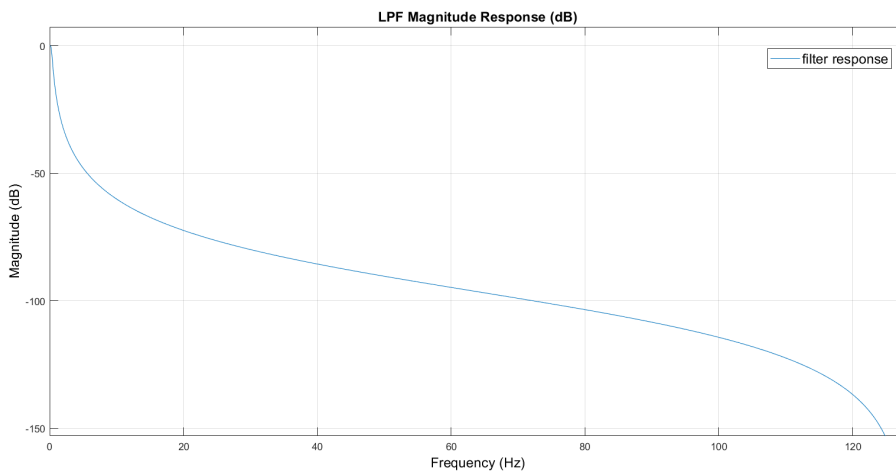


Figure 4.7 – Frequency response for Low Pass Filter used for envelope extraction in aEEG algorithm.

4.3.3 Envelope Compression

The compact tracing was obtained through the steps of segmentation, terminal point extraction and tracing compression (time and amplitude) (ZHANG and DING, 2013). Thus, in the digital algorithm, the rectified EEG data is acquired with absolute value evaluation. Further, the envelope of the rectified EEG was divided into nonoverlapping epochs of 15-s duration.

The maximum and minimum amplitudes in each epoch are commonly used as the upper and the lower terminal points of the associated reduced segment. Such terminal point is defined near (but not at) the upper/lower edge of the epoch (ZHANG and DING, 2013). In the present study, the position of the selected terminal point in the sorted data was acquired from the 10 and 90 percentiles obtained for each segment. Such percentiles meet the definition of the terminal position as a percentage near and <100% for the upper limit and percentage near and >0% for the lower limit. The use of this percentiles intent to avoid outlier high-amplitude and low-amplitude noise values (ZHANG and DING, 2013).

Finally, the compression of envelope was achieved in the scales of time (x -axis) by laterally compressing the tracing (time-scale reference: 6cm/h) and amplitude (y -axis) by drawing it with a base-10 log-scale. The applied scale is showed below:

$$g(y) = \begin{cases} y & ,y \leq 10 \\ \log(y) \times 10 & ,y > 10 \end{cases} \quad (4.1)$$

where, y and $g(y)$ are respectively the magnitude of the signal expressed in μV and graphic unities. Therefore, the range of 0-100 μV corresponds to a range of 0-20 in graphic unities (DE MELO, *et al.*, 2015). Such compression aims to reduce the dynamical range of large fluctuations in the raw EEG (e.g., seizures-suppression activities) (ZHANG and DING, 2013). Likewise, values below 10 μV the linear representation gives prominence to depressed cerebral activity with low amplitudes (ZHANG and DING, 2013).

The compression ratio for the acquired signal is then expressed by $\frac{2}{T \times Fs}$, where T is the compression epoch duration (s) and Fs is frequency sampling (Hz). Thus, for a 15-s epoch and $Fs = 256$ Hz, the compression ratio is 0.052%. Accordingly, the time resolution of the compact tracing was 15 s.

The Figure 4.8 shows the signal processing workflow along with the calculation parameters of the aEEG and HaEEG algorithms.

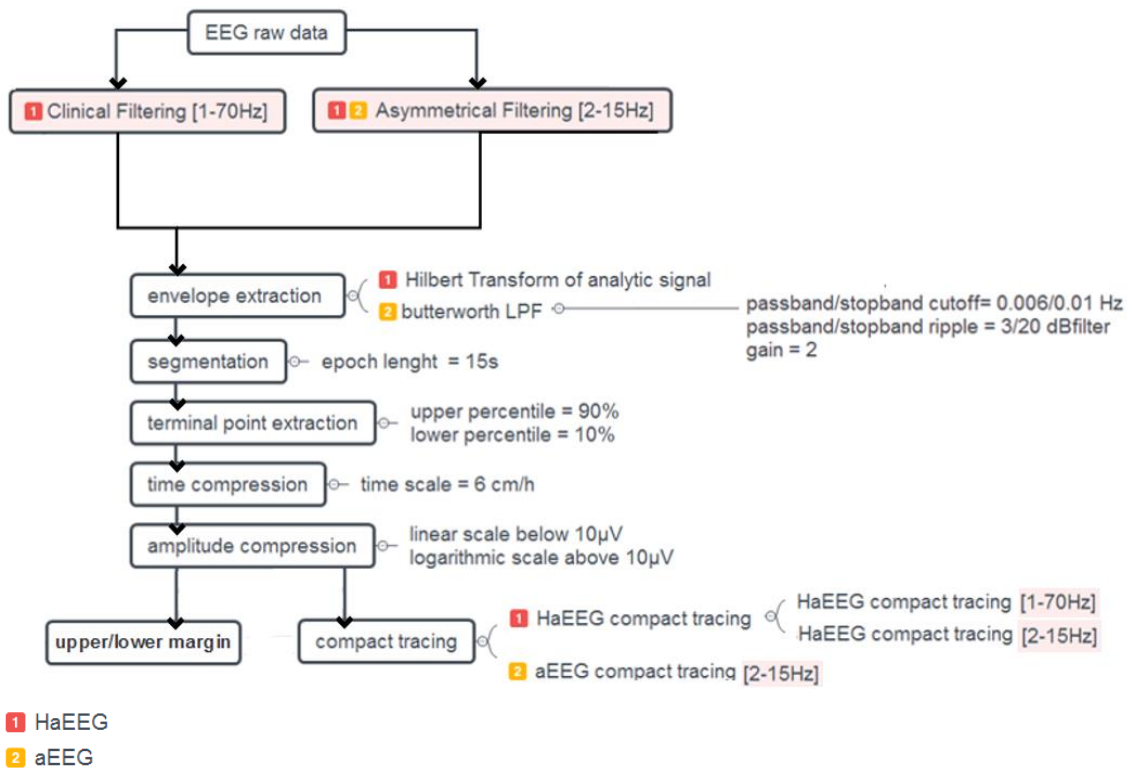


Figure 4.8 – HaEEG (red) and aEEG (yellow) signal processing workflow and calculation parameters of algorithms for analysis within the asymmetrical band filtering (2-15 Hz) and the overall clinical band (1-70 Hz).

4.3.4 Selection of ictal segments

The seizures events were characterized as an abrupt rise in minimum and maximum amplitude. Therefore, the distribution of maximum and minimum margin values was acquired for HaEEG and aEEG compact tracing of seizure and non-seizure epochs (Figure 4.9 to Figure 4.12). Thus, the values of Q1 and Q3 quartiles of each

distribution were used to define upper and lower comparison thresholds. Those quartiles are presented at Table 4.1. The same threshold range was used for HaEEG filtered from 2 to 15 Hz and clinical bands. Similarly, the same threshold range was used for aEEG filtered from 2 to 15 Hz and clinical bands. The upper threshold range for aEEG was slightly narrow than HaEEG, whereas the inverse occurs for the lower threshold range.

Besides, for each patient, each seizure recording was paired with the corresponding annotation file. For each compressed 15-s epoch, the segment was considered as an ictal period if a seizure event lasted for at least 60% of the segment's duration. Therefore, for each threshold pair all the segments acquired for each patient were classified as seizure or non-seizure segment. Further, the occurrence count of those classes was used to obtain the mean sensitivity and specificity for all patients. These parameters were also evaluated by age group. A schematic representation of the classification of segments according to threshold pair values is shown at Figure 4.13.

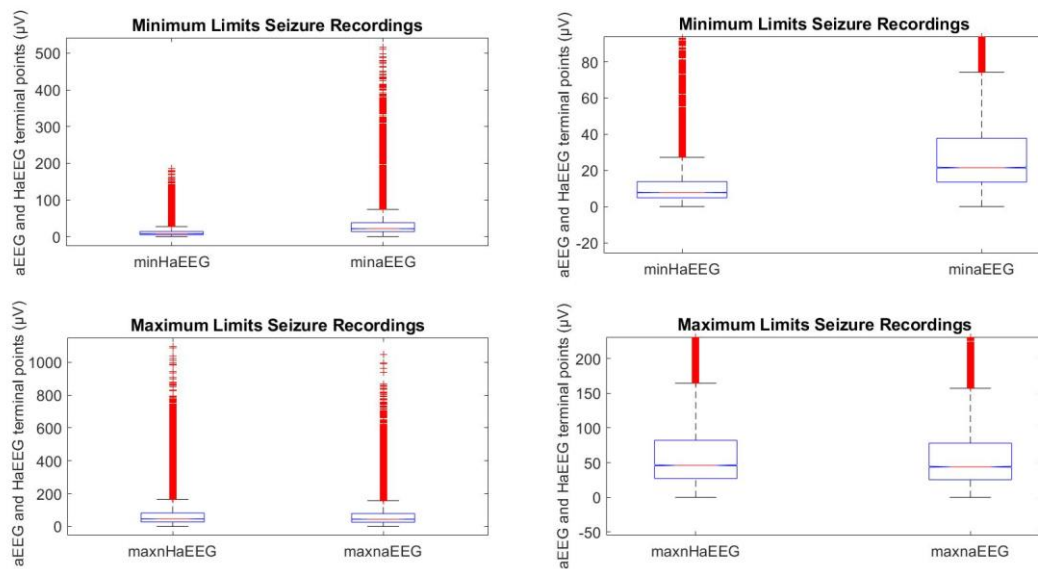


Figure 4.9 – Distribution of maximum (bellow) and minimum (above) margin values of HaEEG and aEEG tracing acquired from for seizure segments filtered from 2 to 15 Hz. Figures at right side are zoomed versions of those at the left side.

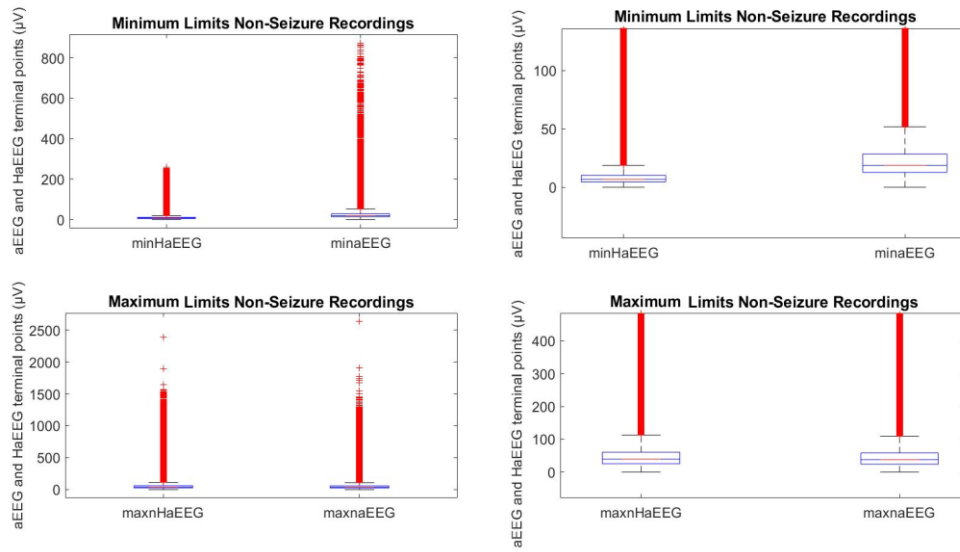


Figure 4.10 – Distribution of maximum (bellow) and minimum (above) margin values of HaEEG and aEEG tracing acquired from for non-seizure segments filtered from 2 to 15 Hz. Figures at right side are zoomed versions of those at the left side.

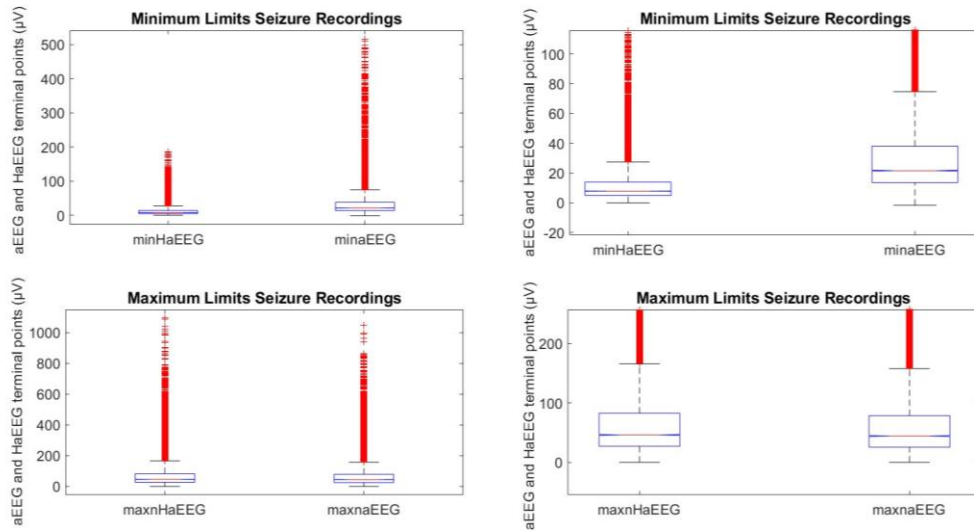


Figure 4.11 – Distribution of maximum (bellow) and minimum (above) margin values of HaEEG and aEEG tracing acquired from for seizure segments filtered from 1 to 70 Hz. Figures at right side are zoomed versions of those at the left side.

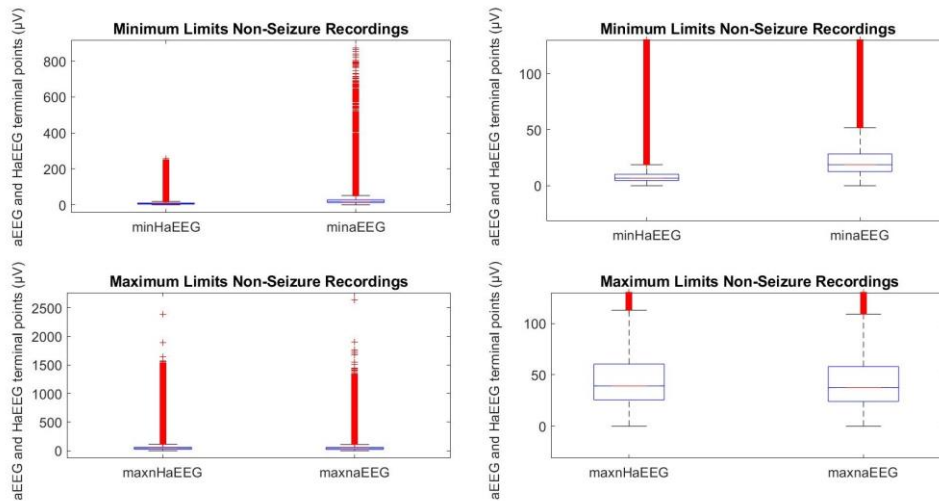


Figure 4.12 – Distribution of maximum (bellow) and minimum (above) margin values of HaEEG and aEEG tracing acquired from for non-seizure recordings filtered from 1 to 70 Hz. Figures at right side are zoomed versions of those at the left side.

Table 4.1 – Quartiles for distribution of maximum and minimum margin of seizure and non-seizure segments

Filtering	Method	Margin	Record Type	Quartile (μV)		
				Q1	Q2	Q3
2 – 15 Hz	HaEEG	Max	NS	4.53	6.70	10.19
			S	27.09	46.06	82.07
		Min	NS	25.61	39.13	60.49
			S	4.85	7.81	13.81
	aEEG	Max	NS	24.09	37.58	58.11
			S	25.42	44.10	78.11
		Min	NS	12.66	18.68	28.27
			S	13.55	21.51	37.81
1 – 70 Hz	HaEEG	Max	NS	25.61	39.13	60.49
			S	27.12	46.19	82.65
		Min	NS	4.53	6.70	10.19
			S	4.86	7.84	13.91

NS = Non-Seizure; S = Seizure.

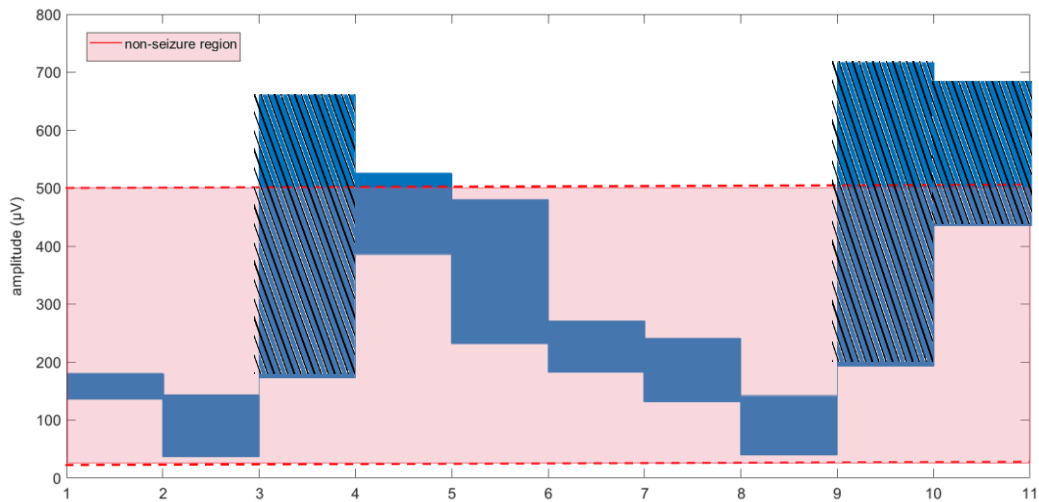


Figure 4.13 – Schematic representation of segment classification according to threshold pair values. Epochs classified as ictal segments were highlighted (dash lines).

4.3.5 Analysis of Instantaneous Frequency

The Hilbert Transform (HT) was also used to estimate the median instantaneous frequency (IF) of each 15-s compressed epoch. Therefore, the IF was obtained for each segment and median these frequencies were acquired and classified according to the corresponding annotation file for each subject. The analysis of the distribution of these medians were performed for seizure and non-seizure segments. Thereafter, the non-parametric Wilcoxon Rank Sum Test was used to evaluate the null hypothesis of equal medians for those two groups. This method was pursued for the signals acquired from the asymmetrical filtering (2-15 Hz) and for those filtered at the overall clinical bands (1-70 Hz).

5 RESULTS

5.1.1 Selection of ictal segments

The HaEEG maximum mean accuracy (16.75 %) at the asymmetrical filtered band (2-15 Hz) was acquired for the range defined by minimum amplitude $> 12.15 \mu\text{V}$ and maximum amplitude $< 30 \mu\text{V}$. Thus, a mean sensitivity of 98.18% and a mean specificity of 5.54 % were found for this range.

Besides, the maximum mean accuracy (12.54 %) of HaEEG for the clinical band filtering (1-70 Hz) was also found for the voltage range with lower amplitude $> 12.15 \mu\text{V}$ and upper amplitude $< 30 \mu\text{V}$. Further, for values of upper threshold higher than $80 \mu\text{V}$ extremely poor sensitivity values (near to 0 %) were acquired for both filtering ranges. Thus, the ROC classification performance for both filtering ranges is shown at Figure 5.1.

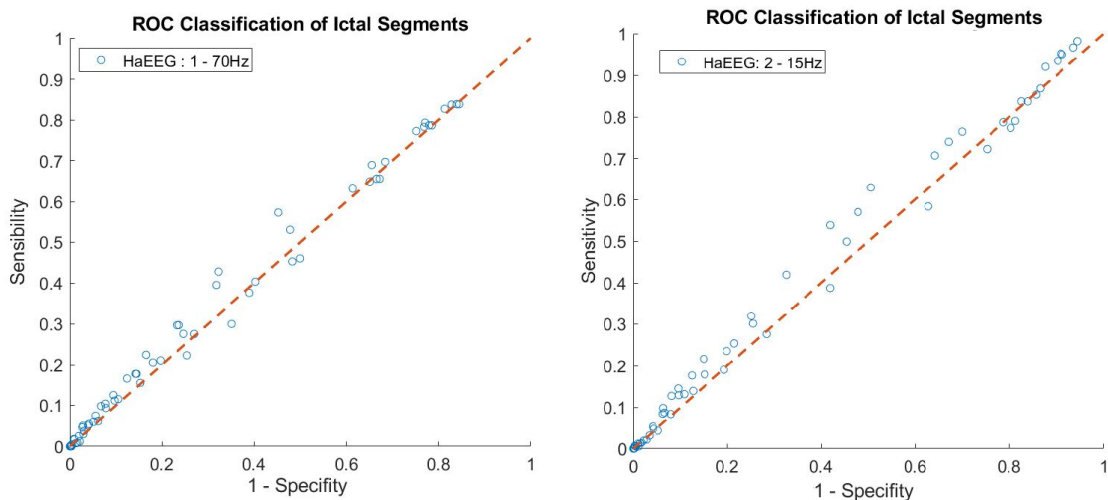


Figure 5.1 – ROC Classification of Ictal HaEEG segments of all subjects for signals filtered within 1-70 Hz (left) and 2-15 Hz (right).

Further, the classification of ictal segments performed with aEEG method (Figure 5.2) for asymmetrical band filtering acquired the maximum mean accuracy (14.50 %) for the voltage range with lower amplitude above $12.15 \mu\text{V}$ and upper amplitude lower than $25 \mu\text{V}$.

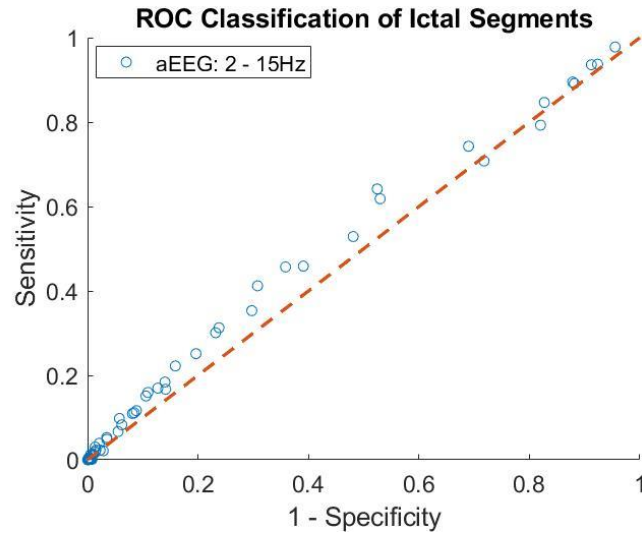


Figure 5.2 – ROC Classification of Ictal aEEG segments for all subjects for signals with asymmetrical filtering.

Accordingly, the maximum and minimum values of mean accuracy, mean specificity and mean sensibility for both methods and filtering ranges are summarized at Table 5.1.

Table 5.1 – Summarized performance metrics for aEEG and HaEEG methods.

Filtering	Method	Margin (μV)		Performance metric			
		Upper	Lower	Min/Max	Acc (%)	Sen (%)	Spe (%)
2 – 15 Hz	HaEEG	< 25	> 12.15	Max	16.75	98.18	05.54
		< 300	> 12.15	Min	0.996	0	99.86
	aEEG	< 25	> 12.15	Max	14.50	97.80	04.48
		< 500	> 12.15	Min	0.996	0	99.84
1 – 70 Hz	HaEEG	< 30	> 12.15	Max	12.54	83.84	99.67
		< 150	> 6.97	Min	0.994	0	16.08

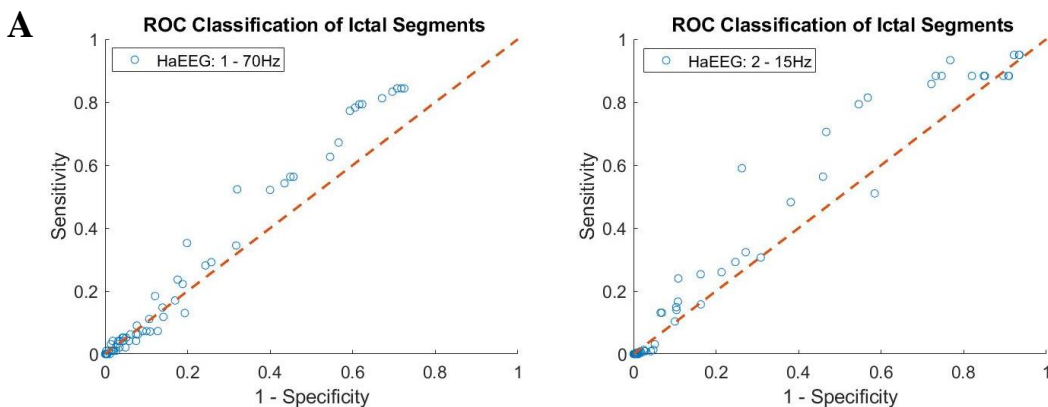
Acc = Accuracy, Sen = Sensibility, Spe = Specificity

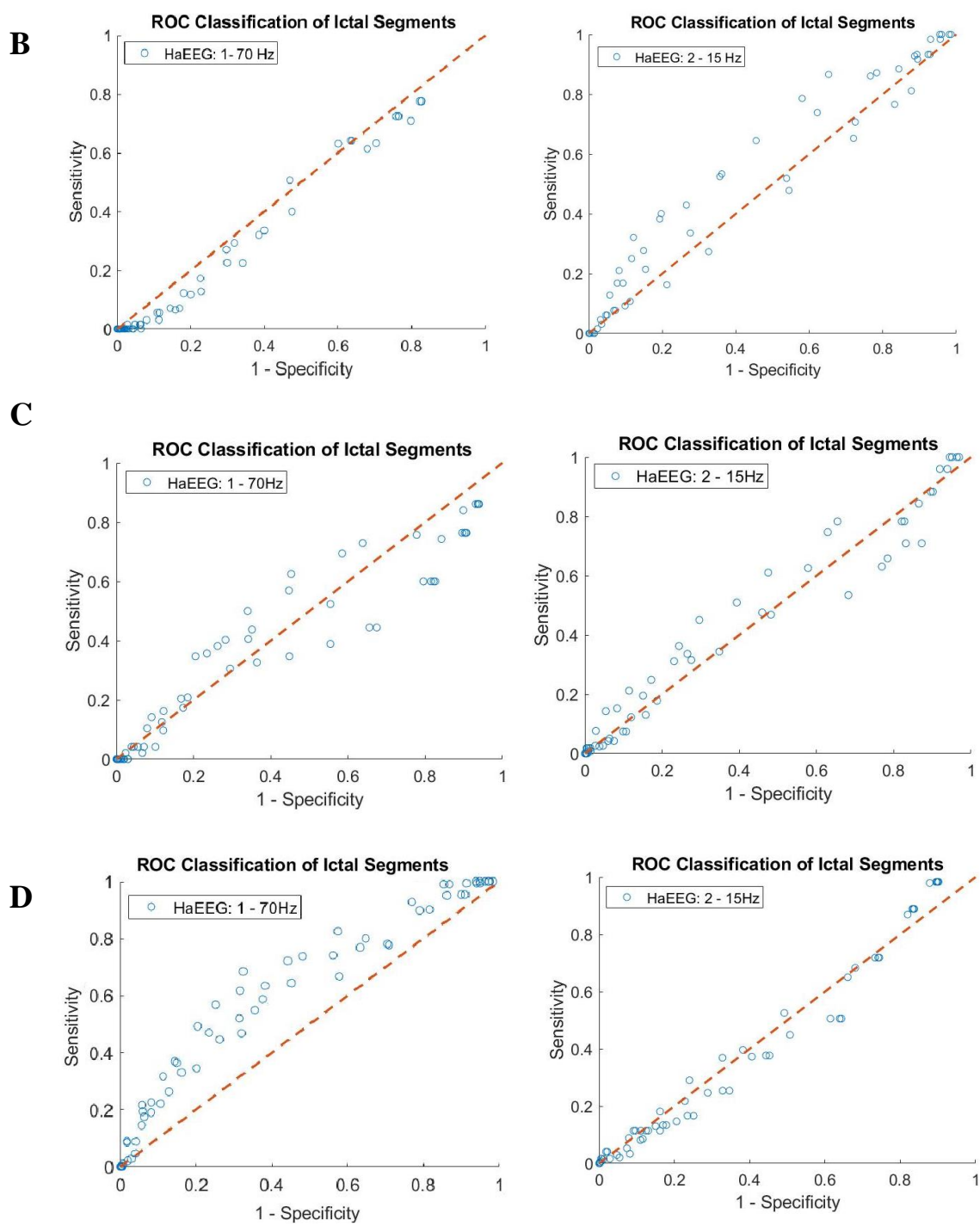
Therefore, as shown at Table 5.1, the maximum mean accuracy was found for the voltage range within the lower amplitude $> 12.15 \mu\text{V}$ and upper amplitude $< 25-30 \mu\text{V}$ for both methods and filtering bands. Nevertheless, minimum mean accuracy was found within different voltage ranges according to the method evaluated.

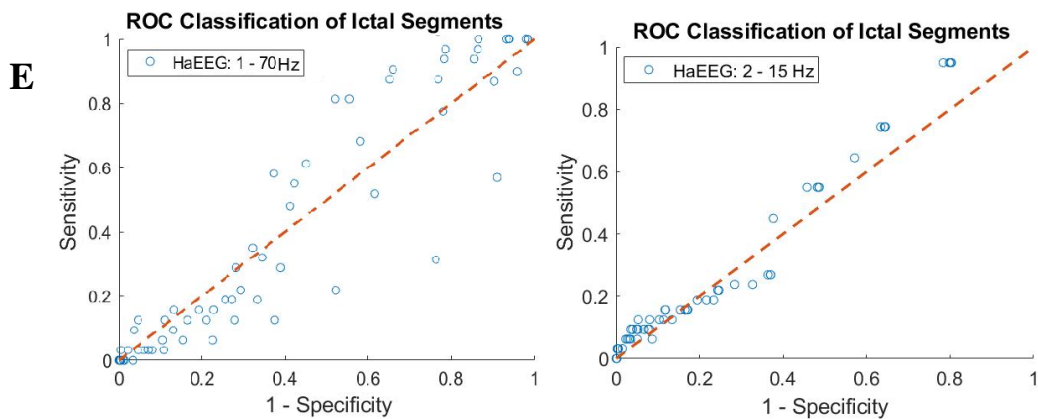
Furthermore, the analysis of mean accuracy within age groups (Figure 5.3 and Figure 5.4) presents different performances and optimum voltage ranges.

Thus, the HaEEG highest accuracy (44.10 %) at the asymmetrical filtered band (2-15 Hz) was acquired for was obtained for 13-16 years group. Such performance was acquired for the voltage range with lower amplitude $> 6.95 \mu\text{V}$ and upper amplitude $< 25 \mu\text{V}$. Meanwhile, the lowest accuracy (9.56 %) value was found for the 10-12 years age groups. Such performance was acquired for the voltage range of the lower margin $> 10.85 \mu\text{V}$ and the upper margin $< 30 \mu\text{V}$.

Thereafter, the highest accuracy (29.56 %) of HaEEG for the clinical band filtering was found for the 13-16 years group at the voltage range with lower amplitude $> 8.9 \mu\text{V}$ and upper amplitude $< 30 \mu\text{V}$. Besides, the lowest accuracy values were found for 6-9 years (7.17 %) and 10-12 years (7.47 %) age groups. Such performance were acquired for the voltage range within the lower margin $> 12.15 \mu\text{V}$ and the upper margin $< 40 \mu\text{V}$ for both age groups.

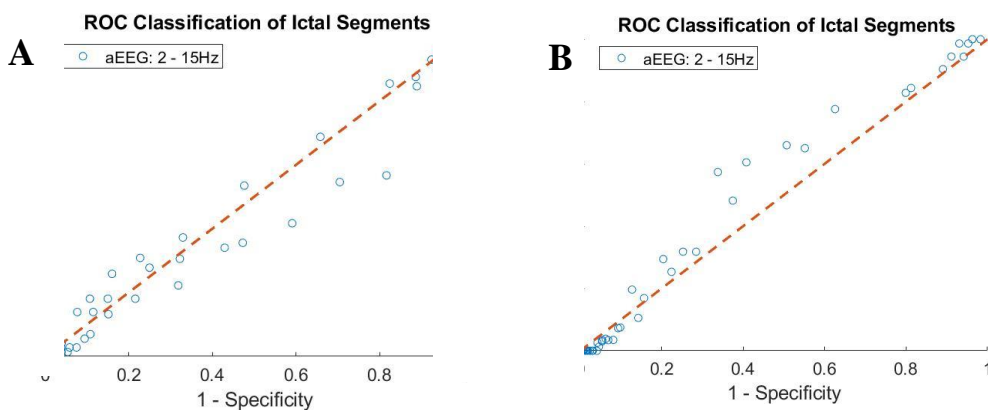






E Figure 5.3 – ROC Classification of Ictal segments according to age group for HaEEG for signals filtered within 1-70 Hz (left) and 2-15 Hz (right). A. subjects of 1.5-3.5 years age group. B. subjects of 6-9 years age group; C. subjects of 10-13 years age group; D subjects of 14-16 years age group; E. subjects of 18-19 years age group.

Similarly, the highest accuracy (28.56 %) acquired with aEEG method (Figure 5.4) for asymmetrical band filtering was found for the 13-16 age group at the voltage range with lower amplitude $> 10.85 \mu\text{V}$ and upper amplitude $< 25 \mu\text{V}$. Likewise, the lowest accuracy (7.89 %) was acquired for the 10-12 years age group within the voltage range of minimum margin $> 12.15 \mu\text{V}$ and maximum margin $< 25.00 \mu\text{V}$.



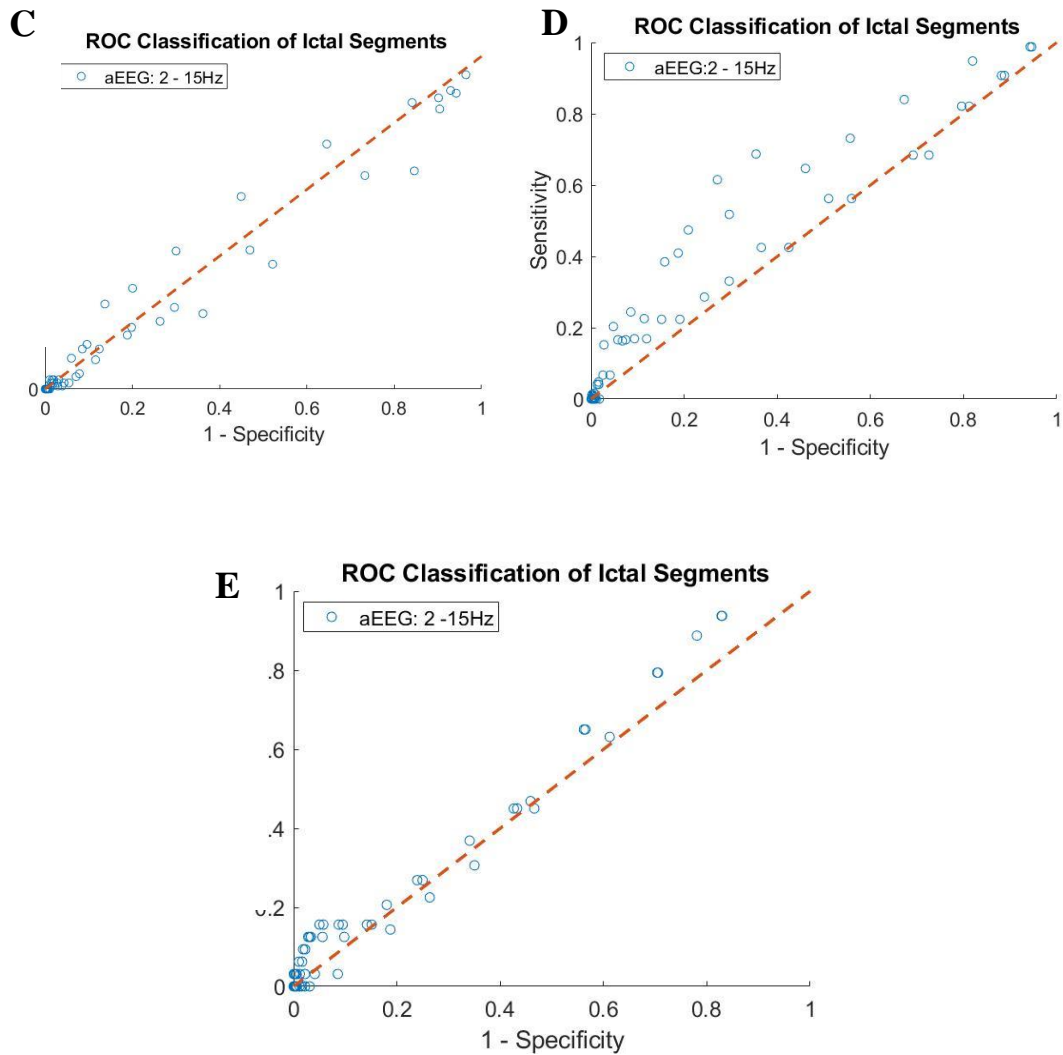


Figure 5.4 – ROC Classification of Ictal segments according to age group for aEEG with asymmetrical filtering 2-15 Hz. A. subject of 1.5-3.5 years age group. B. subjects of 6-9 years age group; C. subjects of 10-13 years age group; D subjects of 14-16 years age group; E. subjects of 18-19 years age group.

Accordingly, the maximum and minimum values of accuracy, mean specificity and mean sensibility for both methods and filtering ranges within each age group are summarized at Table 5.2.

Table 5.2 – Summarized performance metrics for aEEG and HaEEG methods analyzed with asymmetrical filtering and clinical band filtering for each age group.

Filtering	Method	Age group	Margin (μV)		Performance metric			
			Upper	Lower	Min/Max	Acc (%)	Sen (%)	Spe (%)
2 – 15 Hz	HaEEG	1.5-3	< 40	> 12.15	Max	13.28	95.00	07.85
			< 80	> 6.95	Min	0.984	0	98.74
		6-9	< 30	> 10.85	Max	13.25	1	04.52
			< 100	> 5.65	Min	0.983	0	98.48
		10-12	< 30	> 10.85	Max	9.555	1	05.49
			< 150	> 8.9	Min	0.993	0	99.43
		13-16	< 25	> 6.95	Max	44.10	98.33	10.49
			< 300	> 12.15	Min	0.994	0	99.83
		18-19	< 25	> 5.65	Max	12.72	95.00	21.66
			< 200	> 12.15	Min	0.996	0	99.81
	aEEG	1.5-3	< 25	> 12.15	Max	8.03	97.92	02.94
			< 60	> 6.95	Min	0.985	0	98.64
		6-9	< 30	> 12.15	Max	12.37	1	03.71
			< 40	> 6.95	Min	0.958	0	95.94
		10-12	< 25	> 12.15	Max	7.89	94.44	03.57
			< 60	> 6.95	Min	0.988	0	98.97
		13-16	< 25	> 10.85	Max	28.56	98.78	05.73
			< 25	> 5.65	Min	0.979	0	98.19
		18-19	< 25	> 10.85	Max	12.17	93.75	17.16
			< 25	> 5.65	Min	0.967	0	96.89
1 – 70 Hz	HaEEG	1.5-3	< 35	> 12.15	Max	8.63	84.36	98.84
			< 200	> 6.95	Min	0.986	0	29.24
		6-9	< 40	> 12.15	Max	7.17	77.57	93.56
			< 50	> 6.95	Min	0.934	0	17.79
		10-12	< 40	> 12.15	Max	7.47	86.11	96.99
			< 70	> 5.65	Min	0.969	0	6.91

Filtering	Method	Age group	Margin (μV)		Performance metric			
			Upper	Lower	Min/Max	Acc (%)	Sen (%)	Spe (%)
1 – 70 Hz	HaEEG	13-16	< 30	> 8.90	Max	29.56	0	99.47
			< 200	> 10.85	Min	0.991	98.80	6.22
		18-19	< 35	> 12.15	Max	10.63	0	96.68
			< 50	> 6.95	Min	0.966	1	13.49

Acc = Accuracy, Sen = Sensibility, Spe = Specificity

Further, as shown at Table 5.2, the use of asymmetrical filtering achieves performances consistently higher when compared with clinical filtering strategy. Thus, HaEEG highest accuracy achieved for within 13-16 years age group was higher using asymmetrical filtering (44.10 %) than applying clinical filtering (29.56 %). However, the minimum accuracy values were found within different voltage ranges according to the method and age group evaluated.

5.1.2 Analysis of Instantaneous Frequency

The distribution of median instantaneous frequency (IF) for ictal and non-ictal periods shows a median of 3.65 Hz for seizure records and 3.55 Hz for non-seizure records. Moreover, non-seizure segments contain more outliers than the ictal periods. Accordingly, this occurrence is more preminent for segments acquired using 1 to 70 Hz. Subsequently, the difference between ictal and non-ictal median IF based on Wilcoxon Rank Sum Test was significant for signals filtered from 2-15 Hz ($p = 0.0055$) but not for signals filtered from 1-70 Hz ($p = 0.1816$).

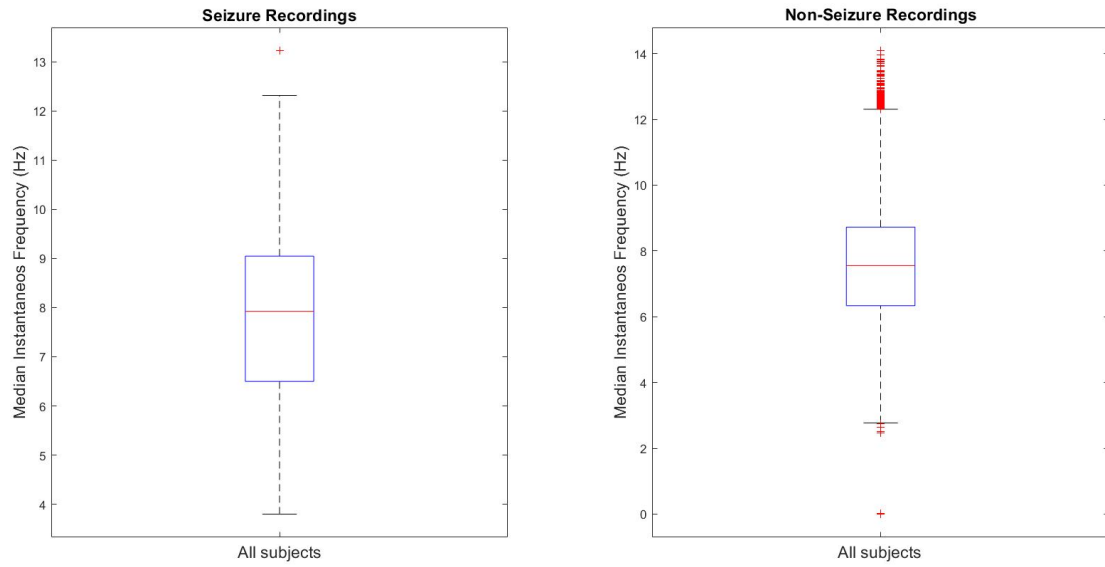


Figure 5.5 – Distribution of median of instantaneous frequencies acquired from for seizure (left) and non-seizure segments (right) recordings filtered from 2 to 15 Hz.

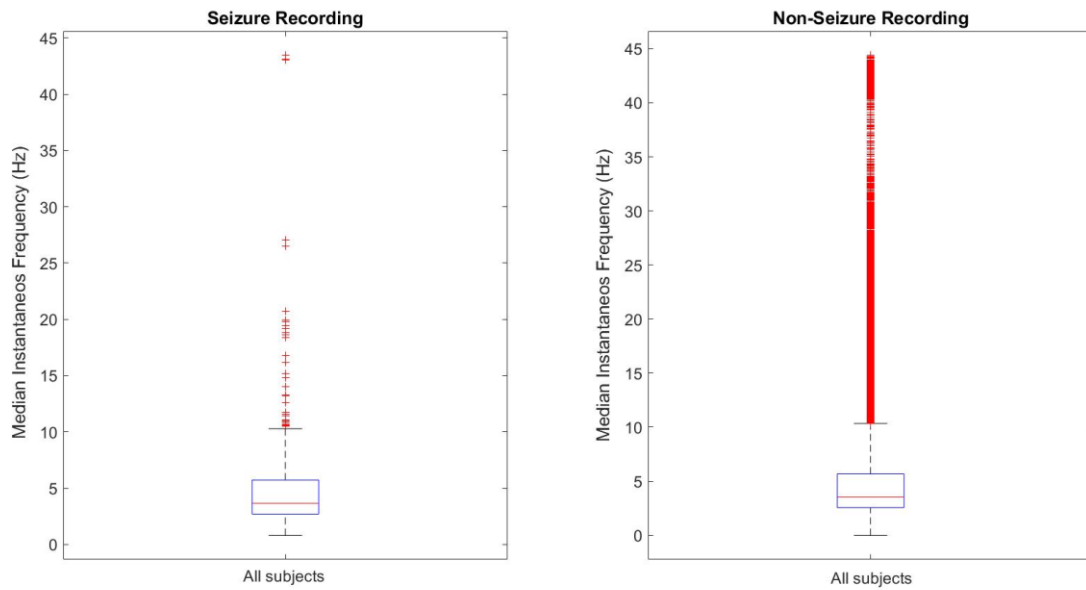


Figure 5.6 – Distribution of median of instantaneous frequencies acquired from for seizure (left) and non-seizure segments (right) recordings filtered from 1 to 70 Hz.

5.1.3 Electroencephalogram Data Platform

An integration architecture for EEG analysis was developed according to the design scheme presented in Figure 4.2. A condensed relational scheme of this database is presented at Figure 5.7.

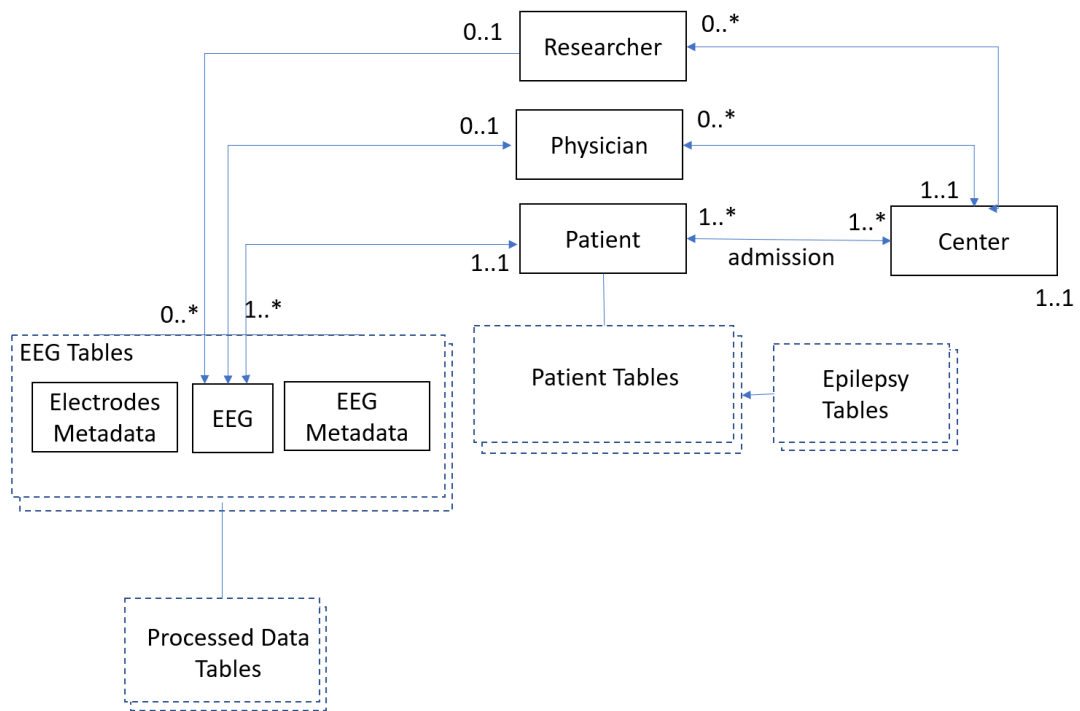


Figure 5.7 – Database design scheme.

Accordingly, at the condensed scheme presented at Figure 5.7, the dotted containers represent groups of related tables while rectangles represent tables. The relations between table groups and tables are expressed by connecting arrows along with the cardinality and ordinality of the relationship. Those two properties express respectively maximum and minimum number of relationships.

Therefore, patient tables group retain comprehensive data about patients' history. Likewise, epilepsy tables groups hold description and classification about epilepsies' and syndromes' types. Further, pre-processed records related information is retained at EEG tables group, which holds information of record montage, annotation, channel and metadata. Furthermore, the admission relationship is also stored in a table.

Besides, processed data tables group holds information about the features calculated from EEG data along with the signal processing methods and parameters applied to perform the calculation.

This database is available from a client application software (Figure 5.8) that allows data input, browsing and querying the available the dataset.

The image shows a web-based patient registration form titled "REGISTRO DE PACIENTE". The form is set against a light gray background with a blue header bar at the top right containing a "Sair" button and a menu icon. The form fields are organized as follows:

- Nome**: Text input field.
- Sobrenome**: Text input field.
- Nascimento**: Three dropdown menus for day, month, and year.
- Sexo**: Dropdown menu.
- Peso**: Text input field.
- Altura**: Text input field.
- Nº cartão SUS/Convênio**: Text input field.
- CPF**: Text input field.
- RG**: Text input field.
- Emissor**: Text input field.
- Nº Prontuário**: Text input field.
- Nº Estudo**: Text input field.
- Email**: Text input field.
- Telefone**: Text input field.
- Uso de Medicamentos**: Radio buttons for "Não" and "Sim", followed by a text input for "Nome do Medicamento".
- Síndrome epilética conhecida**: Radio buttons for "Não" and "Sim", followed by a text input for "Nome da Síndrome".
- Traumatismo Craniano**: Radio buttons for "Não" and "Sim", followed by a text input for "Evento".
- Comorbidades**: Radio buttons for "Não" and "Sim", followed by a text input for "Nome da Comorbidade".

Figure 5.8 – Example of register form of Database client application.

6 DISCUSSION

An architecture was designed to handle the insertion, processing, and analysis of EEG data. Such integration platform is still in development and could be used to integrate health care centers to research facilities such as university centers. The increasing number of database and integration efforts highlights the importance of a publicly available EEG data for seizure prediction and related research communities. Moreover, storage of analytical information can enhance application of machine learning application and combination of features from different algorithms (IHLE *et al.*, 2012).

Hence, this architecture was used to evaluate epileptic seizure detection performances of aEEG and HaEEG methods based on accuracy, specificity and sensibility values. Thus, albeit such detection method presented suitable sensitivity values, it also presented low specificity rates. Nonetheless, a heterogeneous dataset was evaluated regarding factors as patients age, epilepsy syndrome, electrode montage and number, whilst, in this study, the same classification thresholds were used for all of them. Information about seizure type and location were not available. Such parameters are referred as EEG sensitivity intervenors (PILAI *et al.*, 2006).

In this context, such wide range of age can be not be adequate for voltage criterion evaluation since the EEG tracing matures from birth to young adulthood (NIEDERMEYER and SILVA, 2005). Then, childhood EEG presents more variability (spontaneous change in the EEG seen over time) than the adult. Accordingly, NIEDERMEYER *et al.* (2005) reports that is often difficult to define whether a deviant pattern is a sign of immaturity or brain disorder.

Besides, enhance of detection rates are expected for high-frequency, long lasting and central region-generated seizures with the combined application of aEEG and conventional EEG (GLASS *et al.*, 2013; ZHANG e DING, 2013).

Furthermore, an extensive literature review is available for aEEG voltage criterion patterns and evaluation of the method accuracy, sensitivity and specificity. Thus, the use of normative values of amplitudes of the aEEG have been helpful to assess neonatal normal development (HELLSTRÖM-WESTAS *et al.*, 2006). However,

great number of such studies is based on observation and test of neonatal EEG or Hypoxic Ischemic Encephalopathy (HIE) (HELLSTRÖM-WESTAS *et al.*, 2006; 2008). Meanwhile, there is still a lack of studies on evaluation of aEEG and HaEEG obtained from conventional multichannel EEG.

In addition, Hellström-Westas and colleagues (2006) also report that caution must be taken when interpreting amplitude of the EEG. Although this measurement is very important, it may be affected by a variety of factors such as interelectrode distance, scalp edema, and frequency noise (HELLSTRÖM-WESTAS *et al.*, 2006).

Thereafter, the use of asymmetrical filtering (2-15 Hz) and overall clinical band (1-70 Hz) was also compared. Then, the use of asymmetrical filtering achieves performances consistently higher when compared with clinical filtering strategy.

Moreover, this study also aimed to evaluate the instantaneous frequency as a parameter for selection of ictal and non-ictal segments. Thus, the difference between ictal and non-ictal median assessed from Wilcoxon Rank Sum Test was significant for the HaEEG filtered from 2-15 Hz but not for signals filtered from 1-70 Hz. Indeed, instantaneous frequency obtained from Hilbert Transform is supposed to provide better results for signals with narrower band. Accordingly, WITTE and colleagues reported a higher envelope magnitudes and low variance of the instantaneous frequency for epileptic spikes epochs analyzed with Discrete Hilbert Transform (WITTE *et al.*, 1991).

7 CONCLUSION

7.1 PURPOSE AND CONTRIBUTION

The present work proposed the application of reduction EEG signal processing techniques to signals organized within a developed EEG database. For this goal a platform integration and a database were designed and will remain available for research and collaboration among neuroengineering community, such that should be used to facilitate signal processing and, possibly, big data analysis.

Besides a preliminary evaluation of HaEEG accuracy, sensitivity and specificity for a detection method based on voltage criterion was also carried on. Such investigation presented suitable mean sensitivity values (HaEEG = 98.18 %; aEEG = 97.80 %), but poor specificity values. Thus, a higher accuracy was obtained for the HaEEG using asymmetrical filtering. The results also support different sensitivity values within different age groups. Accordingly, the analysis of median instantaneous frequency also shows statistical difference between ictal and non-ictal periods for segments acquired from asymmetrical filtering ($p = 0.0055$), but not at the 1-70 Hz band.

7.2 FUTURE WORK

The integration platform presented in this study is still under development, as more signal process methods can be added to process flow. Further, the storage of EEG extracted features may contribute to implementation of comprehensive machine learning models and subsequent evaluation of them. Therefore, collaborative studies with health care facilities and universities centers can help to provide quality EEG data and information for cross validation of prediction methods.

Furthermore, the evaluation of HaEEG voltage criterion within different and narrow age ranges should still be performed. Similarly, comparison of HaEEG and aEEG for highly reported pathological patterns, such as neonatal HIE, can bring comprehension on HaEEG patterns analysis.

8 BIBLIOGRAPHY

AGARWAL, R. *et al.* Automatic EEG analysis during long-term monitoring in the ICU. **Electroencephalography and clinical Neurophysiology**, v. 107, n. 1, p. 44–58, 1998.

AHMED, B.; TAFRESHI, R.; LANGARI, R. The Future of Automatic EEG Monitoring in the Intensive Care. In: 2008 International Conference on BioMedical Engineering and Informatics. IEEE, v. 2, p. 520-524, 2008.

AICARDI, J.; TAYLOR, D. C. History and Physical Examination. *In*: ENGEL, J.; PEDLEY, T. A. (Eds.). **Epilepsy: a comprehensive textbook**. 2 ed USA: Lippincott Williams & Wilkins, v. I, 2008.

AL NAQEEB, N. *et al.* Assessment of neonatal encephalopathy by amplitude-integrated electroencephalography. **Pediatrics**, v. 103, n. 6, p. 1263–1271, 1999.

ALOTAIBY, T. N. *et al.* EEG seizure detection and prediction algorithms: a survey. **EURASIP Journal on Advances in Signal Processing**, v. 2014, n. 1, p. 183, 2014.

ANDRZEJAK, R. G. *et al.* Indications of nonlinear deterministic and finite-dimensional structures in time series of brain electrical activity: Dependence on recording region and brain state. **Physical Review E**, v. 64, n. 6, 20 nov. 2001.

BENDAT, J. S.; PIERSOL, A. G. **Random Data**. Hoboken, New Jersey, Wiley Series in Probability and Statistics, 2010.

BENICZKY, S. *et al.* Standardized computer-based organized reporting of EEG: SCORE. **Epilepsia**, v. 54, n. 6, p. 1112–1124, 2013.

BHARUCHA, N. E.; CARPIO, A.; DIOP, A. G. Epidemiology in Developing Countries. *In*: ENGEL, J.; PEDLEY, T. A. **Epilepsy: A Comprehensive Textbook, 2nd Edition**. USA: Lippincott Williams & Wilkins, v. I, 2008.

BLUM, A. S.; RUTKOVE, S. B. **The Clinical Neurophysiology Primer**. New Jersey: Human Press, 2007.

BOASHASH, B. Estimating and interpreting the instantaneous frequency of a signal. I. Fundamentals. **Proceedings of the IEEE**, v. 80, n. 4, p. 520–538, 1992.

BOUREZ-SWART, M. D. *et al.* Detection of subclinical electroencephalographic seizure patterns with multichannel amplitude-integrated EEG in full-term neonates. **Clinical Neurophysiology**, v. 120, n. 11, p. 1916–1922, 2009.

BURNEO, J. G.; TELLEZ-ZENTENO, J.; WIEBE, S. Understanding the burden of epilepsy in Latin America: A systematic review of its prevalence and incidence. **Epilepsy Research**, v. 66, n. 1, p. 63–74, 1 ago. 2005.

BUZSÁKI, G.; TRAUB, R. D. Physiologic Basis of the Electroencephalogram and Local Field Potentials. *In*: ENGEL, J.; PEDLEY, T. A. (Eds.). **Epilepsy: a comprehensive textbook**. USA: Lippincott Williams & Wilkins, v. 1, 2008.

DE MELO, T. M.; CAGY, M.; INFANTOSI, A. F. C. **Aplicação da transformada de Hilbert para redução do eletroencefalograma multicanal de longa duração**. Anais do XXIV Congresso Brasileiro em Engenharia Biomédica. 2014. Disponível em:

<http://www.canal6.com.br/cbeb/2014/artigos/cbeb2014_submission_541.pdf>. Acesso em: 24 nov. 2017

DE MELO, T. M.; INFANTOSI, A. F. C.; CAGY, M. **Aplicação da Transformada de Hilbert e Separação em Bandas Clínicas para Redução do Eletroencefalograma de Longa Duração**. Rio de Janeiro: Universidade Federal do Rio de Janeiro, COPPE, Programa de Engenharia Biomédica, 2015.

DOS SANTOS, T. E. B.; CAGY, M. **Redução do Eletroencefalograma durante monitorização contínua de paciente crítico**. Rio de Janeiro: Universidade Federal do Rio de Janeiro, COPPE, Programa de Engenharia Biomédica, mar. 2017.

EL-DIB, M. *et al.* Amplitude-integrated electroencephalography in neonates. **Pediatric neurology**, v. 41, n. 5, p. 315–326, 2009.

ENGEL, J. A Proposed Diagnostic Scheme for People with Epileptic Seizures and with Epilepsy: Report of the ILAE Task Force on Classification and Terminology. **Epilepsia**, v. 42, n. 6, p. 796–803, 20 dez. 2001.

ENGEL, J.; PEDLEY, T. A. **Epilepsy: A Comprehensive Textbook**. 2 ed ed. USA: Lippincott Williams & Wilkins, v. I, 2008.

EVANS, E. *et al.* Accuracy of amplitude integrated EEG in a neonatal cohort. **Archives of Disease in Childhood-Fetal and Neonatal Edition**, v. 95, n. 3, p. F169–F173, 2010.

FELDMAN, M. Time-varying vibration decomposition and analysis based on the Hilbert transform. **Journal of Sound and Vibration**, v. 295, n. 3, p. 518–530, 22 ago. 2006.

FELDMAN, S. A.; ELLIS, H. **Principles of resuscitation**. Blackwell, 1967.

FERNANDES, J. G.; SCHMIDT, M. I. **Epidemiologia das Crises Epilépticas em Porto Alegre: Um Estudo Populacional**. Porto Alegre: Universidade Federal do Rio Grande do Sul, 1993.

FISHER, R. S. *et al.* Epileptic Seizures and Epilepsy: Definitions Proposed by the International League Against Epilepsy (ILAE) and the International Bureau for Epilepsy (IBE). **Epilepsia**, v. 46, n. 4, p. 470–472, abr. 2005.

FISHER, R. S. *et al.* ILAE official report: a practical clinical definition of epilepsy. **Epilepsia**, v. 55, n. 4, p. 475–482, 2014.

FISHER, R. S. *et al.* Operational classification of seizure types by the International League Against Epilepsy: Position Paper of the ILAE Commission for Classification and Terminology. **Epilepsia**, v. 58, n. 4, p. 522–530, abr. 2017.

FISHER, R. S.; SCHARFMAN, H. E.; DECURTIS, M. How can we identify ictal and interictal abnormal activity? *In: Issues in Clinical Epileptology: A View from the Bench*. Springer, 2014. p. 3–23.

FREEMAN, W. J. Hilbert transform for brain waves. **Scholarpedia**, v. 2, n. 1, p. 1338, 15 jan. 2007.

GIBBS, F. A.; DAVIS, H.; LENNOX, W. G. The electro encephalogram in epilepsy and in conditions of impaired consciousness. **American Journal of EEG Technology**, v. 8, n. 2, p. 59–73, 1968.

GLASS, H. C.; WUSTHOFF, C. J.; SHELLHAAS, R. A. Amplitude-integrated electroencephalography: the child neurologist's perspective. **Journal of child neurology**, v. 28, n. 10, p. 1342–1350, 2013.

GOLDBERGER, A. L. *et al.* PhysioBank, PhysioToolkit, and PhysioNet. **Circulation**, v. 101, n. 23, p. e215–e220, 13 jun. 2000.

GUYTON, A. C.; HALL, J. E. **Tratado de fisiologia médica**. Rio de Janeiro, RJ: Elsevier, 2006.

HALFORD, J. J. *et al.* American Clinical Neurophysiology Society Guideline 4: Recording Clinical EEG on Digital Media. **The Neurodiagnostic Journal**, v. 56, n. 4, p. 261-265, 2016.

HARATI, A. *et al.* **The TUH EEG CORPUS: A big data resource for automated EEG interpretation**. 2014 IEEE Signal Processing in Medicine and Biology Symposium (SPMB). IEEE, 2014

HARDIN, A. P. *et al.* Age limit of pediatrics. **Pediatrics**, v. 140, n. 3, p. e20172151, set. 2017.

HAUSER, W. A. Overview: Epidemiology, Pathology, and Genetics. *In*: ENGEL, J.; PEDLEY, T. A. (Eds.). **Epilepsy: a comprehensive textbook**. USA: Lippincott Williams & Wilkins, 2008.

HELLSTRÖM-WESTAS, L. *et al.* Amplitude-integrated EEG Classification and Interpretation in Preterm and Term Infants. **NeoReviews**, v. 7, n. 2, p. e76–e87, 1 fev. 2006.

HELLSTRÖM-WESTAS, L.; DE VRIES, L. S.; ROSÉN, I. **An atlas of amplitude-integrated EEGs in the newborn.** CRC Press, 2008.

HELLSTRÖM-WESTAS, L.; ROSEN, I.; SVENNINGSSEN, N. W. Predictive value of early continuous amplitude integrated EEG recordings on outcome after severe birth asphyxia in full term infants. **Archives of Disease in Childhood-Fetal and Neonatal Edition**, v. 72, n. 1, p. F34–F38, 1995.

HIRTZ, D. *et al.* How common are the “common” neurologic disorders? **How common are the “common” neurologic disorders?**, v. 68, n. 5, p. 326–337, jan. 2007.

HOFFMANN, K. *et al.* Analysis and classification of interictal spike discharges in benign partial epilepsy of childhood on the basis of the Hilbert transformation. **Neuroscience Letters**, v. 211, n. 3, p. 195–198, 1996.

HUANG, N. E. *et al.* The empirical mode decomposition and the Hilbert spectrum for nonlinear and non-stationary time series analysis. **Proceedings of the Royal Society of London. Series A: Mathematical, Physical and Engineering Sciences**, v. 454, n. 1971, p. 903–995, 8 mar. 1998.

HUNTER, M. *et al.* The Australian EEG database. **Clinical EEG and neuroscience**, v. 36, 1 maio 2005.

IHLE, M. *et al.* EPILEPSIAE – A European epilepsy database. **Computer Methods and Programs in Biomedicine**, v. 106, n. 3, p. 127–138, 1 jun. 2012.

ILAE. Proposal for revised clinical and electroencephalographic classification of epileptic seizures. **Epilepsia**, v. 22, n. 4, p. 489–501, 1981.

ILIESCU, C.; CRAIU, D. Diagnostic Approach of Epilepsy in Childhood and Adolescence. **Diagnostic Approach of Epilepsy in Childhood and Adolescence**, *Mædica*. v. 8, n. 2, p. 195–199, jun. 2013.

ILIESCU, C.; CRAIU, D.; DAVILA, C. Diagnostic Approach of Epilepsy in Childhood and Adolescence. v. 8, n. 2, p. 195–199, jun. 2013.

KENNEDY, J. D.; GERARD, E. E. Continuous EEG monitoring in the intensive care unit. **Current neurology and neuroscience reports**, v. 12, n. 4, p. 419–428, 2012.

KING, M. A. *et al.* Epileptology of the first-seizure presentation: a clinical, electroencephalographic, and magnetic resonance imaging study of 300 consecutive patients. **The Lancet**, v. 352, n. 9133, p. 1007–1011, 1998.

KOBAYASHI, K. *et al.* Amplitude-integrated EEG colored according to spectral edge frequency. **Epilepsy research**, v. 96, n. 3, p. 276–282, 2011.

KWAN, P.; SANDER, J. W. The natural history of epilepsy: an epidemiological view. **Journal of Neurology, Neurosurgery & Psychiatry**, v. 75, n. 10, p. 1376–1381, 2004.

LAERHOVEN, H. VAN *et al.* Prognostic Tests in Term Neonates With Hypoxic-Ischemic Encephalopathy: A Systematic Review. **Pediatrics**, v. 131, n. 1, p. 88–98, 1 jan. 2013.

LESSER, R. P.; WEBBER, W. R. S. Principles of Computerized Epilepsy Monitoring. *In*: NIEDERMEYER, E.; SILVA, F. L. D. (Eds.). **Electroencephalography: Basic**

Principles, Clinical Applications, and Related Fields. 5th ed ed. Philadelphia: Wolters Kluwer/ Lippincott Williams & Wilkins Health, 2005. p. 792–796.

LOMMEN, C. M. L. *et al.* An algorithm for the automatic detection of seizures in neonatal amplitude-integrated EEG. **Acta Paediatrica**, v. 96, n. 5, p. 674–680, 2007.

LONG, D. G. Comments on Hilbert transform based signal analysis. 2004.

LOWENSTEIN, D. H.; BLECK, T.; MACDONALD, R. L. It's Time to Revise the Definition of Status Epilepticus. **Epilepsia**, v. 40, n. 1, p. 120–122, jan. 1999.

MARINO, R.; CUKIERT, A.; PINHO, E. Epidemiological aspects of epilepsy in São Paulo, Brazil: a prevalence rate study. **Arquivos de neuro-psiquiatria**, v. 44, n. 3, p. 243–254, 1986.

MARPLE, L. Computing the discrete-time" analytic" signal via FFT. **IEEE Transactions on signal processing**, v. 47, n. 9, p. 2600–2603, 1999.

MAYNARD, D. E.; PRIOR, P. F.; SCOTT, D. F. Device for continuous monitoring of cerebral activity in resuscitated patients. **British medical journal**, v. 4, n. 5682, p. 545, 1969.

MCLACHLAN, R. S. The Canadian Epilepsy Database and Registry. **The Canadian journal of neurological sciences. Le journal canadien des sciences neurologiques**, v. 25, n. S4, p. S27-S31, dez. 1998.

MIZRAHI, E. M.; HRACHOVY, R. A.; KELLAWAY, P. **Atlas of Neonatal Electroencephalography**. 3rd Ed ed. Philadelphia, USA: Lippincott Williams & Wilkins, 2004.

NIEDERMEYER, E.; SILVA, F. L. D. **Electroencephalography: Basic Principles, Clinical Applications, and Related Fields**. 5th ed ed. Philadelphia: Wolters Kluwer/Lippincott Williams & Wilkins Health, 2005.

NITZSCHKE, R. *et al.* Single-channel amplitude integrated EEG recording for the identification of epileptic seizures by nonexpert physicians in the adult acute care setting. **Journal of Clinical Monitoring and Computing**, v. 25, n. 5, p. 329, 19 out. 2011.

OBEID, I.; PICONE, J. The Temple University Hospital EEG Data Corpus. **Frontiers in Neuroscience**, v. 10, 13 maio 2016.

OLESEN, J.; LEONARDI, M. The burden of brain diseases in Europe. **The burden of brain diseases in Europe**, European Journal of Neurology. v. 10, n. 5, p. 471–477, 2003.

OLISCHAR, M. *et al.* Reference values for amplitude-integrated electroencephalographic activity in preterm infants younger than 30 weeks' gestational age. **Pediatrics**, v. 113, n. 1 Pt 1, p. e61–e66, 2004.

OPPENHEIM, A. V.; SCHAFFER, R. W. **Discrete-Time Signal Processing**. 2nd. ed. New Jersey: Prentice Hall, 2010.

PAPOULIS, A. **Signal Analysis**. New York: McGraw-Hill, 1977.

PEDLEY, T. A. EEG Traits. *In*: ENGEL, J.; PEDLEY, T. A. (Eds.). **Epilepsy: A Comprehensive Textbook, 2nd Edition**. USA: Lippincott Williams & Wilkins, 2008. v. I.

PRATI, R. C.; BATISTA, G.; MONARD, M. C. Curvas ROC para avaliação de classificadores. **Revista IEEE América Latina**, v. 6, n. 2, p. 215–222, 2008.

RAMGOPAL, S. *et al.* Seizure detection, seizure prediction, and closed-loop warning systems in epilepsy. **Epilepsy & behavior**, v. 37, p. 291–307, 2014.

RENNIE, J. M. *et al.* Non-expert use of the cerebral function monitor for neonatal seizure detection. **Arch Dis Child Fetal Neonatal**, n. 1st Ed, jan. 2004.

RIZZUTTI, S.; MUSZKAT, M.; CAMPO, C. J. R. DE. Monitorização eletroencefalográfica ambulatorial na epilepsia de difícil controle da infância. **Arquivos de neuro-psiquiatria**, v. 59, n. 4, p. 875–883, 2001.

SALINSKY, M.; KANTER, R.; DASHEIFF, R. M. Effectiveness of multiple EEGs in supporting the diagnosis of epilepsy: an operational curve. **Epilepsia**, v. 28, n. 4, p. 331–334, 1987.

SANDER, J. *et al.* MEDICAL SCIENCE: National General Practice Study of Epilepsy: newly diagnosed epileptic seizures in a general population. **The Lancet**, v. 336, n. 8726, p. 1267–1271, 1990.

SCHEFFER, I. E. *et al.* ILAE classification of the epilepsies: Position paper of the ILAE Commission for Classification and Terminology. **Epilepsia**, v. 58, n. 4, p. 512–521, abr. 2017.

SCHOMER, D. L.; SILVA, F. L. D. **Niedermeyer's Electroencephalography: Basic Principles, Clinical Applications, and Related Fields**. Philadelphia: Wolters Kluwer/Lippincott Williams & Wilkins Health, 2010.

SCOTTISH INTERCOLLEGIATE GUIDELINES NETWORK SIGN. **Diagnosis and management of epilepsy in adults**. Edinburgh: SIGN; 2015, maio. 2015. Disponível em: <<http://www.sign.ac.uk>>. Acesso em: 2 jun. 2019

SEIZURE PREDICTION PROJECT FREIBURG. **Freiburg EEG database**. Disponível em: <<http://epilepsy.uni-freiburg.de/freiburg-seizure-prediction-project/eeg-database>>. Acesso em: 21 maio. 2019.

SHAH, N. A.; WUSTHOFF, C. J. How to use: amplitude-integrated EEG (aEEG). **Archives of Disease in Childhood-Education**, v. 100, n. 2, p. 75–81, abr. 2015.

SHELLHAAS, R. A.; SOAITA, A. I.; CLANCY, R. R. Sensitivity of amplitude-integrated electroencephalography for neonatal seizure detection. **Pediatrics**, v. 120, n. 4, p. 770–777, 2007.

SHOEB, A.; GUTTAG, J. **Application of Machine Learning To Epileptic Seizure Detection**. In: Proceedings of the 27th International Conference on Machine Learning (ICML-10). 2010. p. 975-982

SINHA, S. *et al.* American Clinical Neurophysiology Society Guideline 1: Minimum Technical Requirements for Performing Clinical Electroencephalography. p. 303–307, 2006.

SMITH, D.; DEFALLA, B. A.; CHADWICK, D. W. The misdiagnosis of epilepsy and the management of refractory epilepsy in a specialist clinic. **Qjm**, v. 92, n. 1, p. 15–23, 1999.

SMITH, S. J. M. EEG in the diagnosis, classification, and management of patients with epilepsy. **Journal of Neurology, Neurosurgery & Psychiatry**, v. 76, n. suppl 2, p. ii2–ii7, 2005.

SO, N. K.; BLUME, W. T. The postictal EEG. **Epilepsy & Behavior**, v. 19, n. 2, p. 121–126, 2010.

STEWART, C. P. *et al.* Seizure identification in the ICU using quantitative EEG displays. **Neurology**, v. 75, n. 17, p. 1501–1508, 2010.

TEIXEIRA, C. A. *et al.* EPILAB: A software package for studies on the prediction of epileptic seizures. **Journal of Neuroscience Methods**, v. 200, n. 2, p. 257–271, 2011.

TIAN, G. *et al.* Outcome prediction by amplitude-integrated EEG in adults with hypoxic ischemic encephalopathy. **Clinical neurology and neurosurgery**, v. 114, n. 6, p. 585-589, 2012.

TOET, M. C. *et al.* Amplitude integrated EEG 3 and 6 hours after birth in full term neonates with hypoxic–ischaemic encephalopathy. v. 81, n. 1, p. 19–23, jul. 1999.

TOET, M. C. *et al.* Comparison between simultaneously recorded amplitude integrated electroencephalogram (cerebral function monitor) and standard electroencephalogram in neonates. **Pediatrics**, v. 109, n. 5, p. 772–779, 2002.

TOWNE, A. R. *et al.* Determinants of mortality in status epilepticus. **Epilepsia**, v. 35, n. 1, p. 27–34, 1994.

TRINKA, E. *et al.* A definition and classification of status epilepticus—Report of the ILAE Task Force on Classification of Status Epilepticus. **Epilepsia**, v. 56, n. 10, p. 1515–1523, 2015.

VAN DONSELAAR, C. A. *et al.* Value of the Electroencephalogram in Adult Patients With Untreated Idiopathic First Seizures. **Archives of Neurology**, v. 49, n. 3, p. 231–237, 1 mar. 1992.

VAN DRONGELEN, W. **Signal Processing for Neuroscientists**. 1 ed ed. USA: Academic Press, 2006.

WINTERHALDER, M. *et al.* The seizure prediction characteristics: A general framework to assess and compare seizure prediction methods. **Epilepsy & behavior : E&B**, v. 4, p. 318–25, 1 jul. 2003.

WITTE, H. *et al.* Use of discrete Hilbert transformation for automatic spike mapping: a methodological investigation. **Medical and Biological Engineering and Computing**, v. 29, n. 3, p. 242–248, 1991.

ZHANG, D. *et al.* **Cerebral hypoxic ischemia at different cerebral oxygen saturations in piglets: amplitude-integrated EEG study**. In: 2008 30th Annual

International Conference of the IEEE Engineering in Medicine and Biology Society. IEEE, p. 4712-4715, 2008.

ZHANG, D.; DING, H. Calculation of compact amplitude-integrated EEG tracing and upper and lower margins using raw EEG data. **Health**, v. 5, n. 5, p. 885–891, mai 2013.

ZIVIN, L.; MARSAN, C. A. Incidence and Prognostic Significance of "Epileptiform" Activity in the EEG of Non-Epileptic Subjects: an Assessment of the Histological Changes. **Brain**, v. 91, n. 4, p. 751–778, 1968.

ZWEIG, M. H.; CAMPBELL, G. Receiver-operating characteristic (ROC) plots: a fundamental evaluation tool in clinical medicine. **Clinical chemistry**, v. 39, n. 4, p. 561–577, 1993.

APPENDIX A - Hilbert Transform and Analytic Signal

The analytic signal intent to handle the spectral redundancy by removing the negative frequency side of the signal transform. Thus, the resultant signal preserves all information of the original signal within one-sided spectrum (MARPLE, 1999). Further, the correlation between HT and the analytical signal can be showed from equation 2.1 applying convolution theorem (MARPLE, 1999):

$$\mathcal{F}\{\tilde{x}(t)\} = \mathcal{F}\{\tilde{x}(t)\}\mathcal{F}\left\{\frac{1}{\pi t}\right\}$$

$$\tilde{X}(f) = -iX(f)\text{sgn}(f) \quad (2.11)$$

where *sgn* is sign function:

$$\text{sgn}(x) = \begin{cases} -1, & x < 0 \\ 0, & x = 0 \\ 1, & x > 0 \end{cases} \quad (2.12)$$

Applying definition of sign function below to equation given in 2.11:

$$\tilde{X}(f) = \begin{cases} iX(f), & f < 0 \\ 0, & f = 0 \\ -iX(f), & f > 0 \end{cases} \quad (2.13)$$

Thus,

$$\tilde{X}(f) = -iX(f_+) + iX(f_-) + \quad (2.14)$$

By multiplying both sides of the equation 2.14 by *i*:

$$i\tilde{X}(f) = i[-iX(f_+) + iX(f_-) +]$$

$$i\tilde{X}(f) = X(f_+) + X(f_-) \quad (2.15)$$

Adding $X(f) = X(f_-) + X(f_0) + X(f_+)$ to both sides of the equation above:

$$X(f) + i\tilde{X}(f) = X(f_+) + X(f) - X(f_-)$$

$$X(f) + i\tilde{X}(f) = X(f_+) + X(f_-) + X(f_0) + X(f_+) - X(f_-)$$

$$X(f) + i\tilde{X}(f) = X(f_0) + 2X(f_+) \quad (2.16)$$

The equation above does not present negative frequency components as intended:

$$X(f) = \begin{cases} 2X(f), & f > 0 \\ X(f), & f = 0 \\ 0, & f < 0 \end{cases}$$

$$z(t) = \mathcal{F}^{-1}[Z(f)] \quad (2.17)$$

Thus, applying the equation 2.17 to 2.16

$$X(f) + i\tilde{X}(f) = Z(f) \quad (2.18)$$

Hence, from the Inverse Fourier Transform of the equation 2.18

$$\mathcal{F}^{-1}[X(f)] + i\mathcal{F}^{-1}[\tilde{X}(f)] = \mathcal{F}^{-1}[Z(f)]$$

$$x(t) + i\tilde{x}(t) = z(t) \quad (2.19)$$

Then, applying the definition of HT as an integral to the resultant equation:

$$x(t) + i\mathcal{H}[x(t)] = z(t) \quad (2.20)$$

The acquired signal is complex and the imaginary part of the resultant signal corresponds to the HT of the real part. Likewise, the positive frequency side is multiplied by a 2 factor and thus the resultant analytic signal preserves the original energy (MARPLE, 1999).

APPENDIX B - CHB-MIT EEG Recordings Montage

Table B - Montage used for each CHB-MIT EEG case

Channel Number	Data Set							
	ch01-chb11	ch12-chb14	ch15-1st file	ch15-2nd file-end	chb16-chb21*	chb18 and 19 1st file	chb22	chb23 and 24
1	FP1-F7	FP1-F7	FP1-F7	FP1-F7	FP1-F7	FP1-F7	FP1-F7	FP1-F7
2	F7-T7	F7-T7	F7-T7	F7-T7	F7-T7	F7-T7	F7-T7	F7-T7
3	T7-P7	T7-P7	T7-P7	T7-P7	T7-P7	T7-P7	T7-P7	T7-P7
4	P7-O1	P7-O1	P7-O1	P7-O1	P7-O1	P7-O1	P7-O1	P7-O1
5	FP1-F3							
6	F3-C3	F3-C3	F3-C3	F3-C3	FP1-F3	FP1-F3	FP1-F3	FP1-F3
7	C3-P3	C3-P3	C3-P3	C3-P3	F3-C3	F3-C3	F3-C3	F3-C3
8	P3-O1	P3-O1	P3-O1	P3-O1	C3-P3	C3-P3	C3-P3	C3-P3
9	FP2-F4	FP2-F4	FP2-F4	FP2-F4	P3-O1	P3-O1	P3-O1	P3-O1
10	F4-C4							
11	C4-P4	C4-P4	C4-P4	C4-P4	FZ-CZ	FZ-CZ	FZ-CZ	FZ-CZ
12	P4-O2	P4-O2	P4-O2	P4-O2	CZ-PZ	CZ-PZ	CZ-PZ	CZ-PZ
13	FP2-F8							
14	F8-T8	F8-T8	F8-T8	FP2-F4	FP2-F4	FP2-F4	FP2-F4	FP2-F4
15	T8-P8	T8-P8	T8-P8	T8-P8	F4-C4	F4-C4	F4-C4	F4-C4
16	P8-O2	P8-O2	P8-O2	P8-O2	C4-P4	C4-P4	C4-P4	C4-P4
17	FZ-CZ	FZ-CZ	FZ-CZ	FZ-CZ	P4-O2	P4-O2	P4-O2	P4-O2

Channel Number	Data Set							
	ch01-chb11	ch12-chb14	ch15-1st file	ch15-2nd file-end	chb16-chb21*	chb18 and 19 1st file	chb22	chb23 and 24
18	CZ-PZ		P4-O2					
19	P7-T7	P7-T7	P7-T7		FP2-F8	FP2-F8	FP2-F8	FP2-F8
20	T7-FT9	T7-FT9	T7-FT9	T7-FT9	F8-T8	F8-T8	F8-T8	F8-T8
21	FT9-FT10	T8-P8	T8-P8	F8-T8	T8-P8	T8-P8	T8-P8	FT9-FT10
22	FT10-T8	FT10-T8	FT10-T8	FT10-T8	P8-O2	P8-O2	P8-O2	P8-O2
23	T8-P8			P8-O2				
24		P7-T7	FC1-Ref		P7-T7		P7-T7	
25		T7-FT9	FC2-Ref	P7-T7	T7-FT9			
26		FT9-FT10	FC5-Ref	T7-FT9	FT9-FT10			
27		FT10-T8	FC6-Ref	FT9-FT10	FT10-T8			
28		T8-P8	CP1-Ref	FT10-T8	T8-P8			
29			CP2-Ref	T8-P8	CP2-Ref			
30			CP5-Ref		CP5-Ref			
31			CP6-Ref	FC1-Ref	CP6-Ref			
32				FC2-Ref				
33				FC5-Ref				
34				FC6-Ref				

Channel Number	Data Set							
	ch01- chb11	ch12- chb14	ch15- 1st file	ch15- 2nd file- end	chb16- chb21*	chb18 and 19 1st file	chb22	chb23 and 24
35				CP1- Ref				
36				CP2- Ref				
37				CP5- Ref				
38				CP6- Ref				

**Except for first files of chb18 and 19*

APPENDIX C - CHB-MIT EEG patients summarized information

Table C - CHB-MIT EEG patients and seizure related information per each case

Subject	Gender	Age (years)	Number of seizures	Seizures length (s), ± s.d.
chb01	F	11	7	63.1 (30.5)
chb02	M	11	3	57.3 (41.9)
chb03	F	14	7	57.4 (8.4)
chb05	F	7	5	111.6 (9.4)
chb06	F	1.5	10	15.3 (2.9)
chb07	F	14.5	3	108.3 (30.4)
chb08	M	3.5	5	183.8 (49.2)
chb09	F	10	4	69.0 (7.7)
Chb10	M	3	7	63.9 (17.2)
Chb11	F	12	3	268.7 (418.6)
Chb12	F	2	4	36.9 (16.2)
Chb13	F	3	12	44.6 (21.5)
Chb14	F	9	8	21.1 (8.7)
Chb15	M	16	20	99.6 (53.6)
Chb16	F	7	10	8.4 (2.3)
Chb17	F	12	3	97.7 (15.0)
Chb18	F	18	6	52.8 (14.4)
Chb19	F	19	3	78.7 (2.1)
Chb20	F	6	8	36.8 (6.3)
Chb21	F	13	4	49.8 (28.5)
Chb22	F	9	3	68.0 (8.7)
Chb23	F	6	7	60.6 (32.6)

* Case chb04 was not included in this study because it not fulfill the age criteria for pediatric group.